RDU 090366

DEVELOPMENT OF MICROPUMP IN FUEL CELL APPLICATION USING MICRO ELECTRO-MECHANICAL SYSTEM (MEMS) MACHINING METHOD

(MEMBANGUNKAN PAM MIKRO UNTUK PENGGUNAAN SEL BAHAN API MENGGUNAKAN SISTEM MIKRO ELEKTRO-MECHANICAL (MEMS))

DEVARAJAN RAMASAMY (LECTURER)
MAHENDRAN A/L SAMYKANO (LECTURER)
KUMARAN A/L KADIRGAMA (LECTURER)
LEE GIOK CHUI (LECTURER)
MUHAMAD BIN MAT NOOR (LECTURER)
MAHDHIR BIN MOHD YUSOF (ASSISTANT INSTRUCTOR ENGINEER)

RESEARCH VOTE NO:
RDU 090366

Fakulti Kejuruteraan Mekanikal
Universiti Malaysia Pahang

2010

Fakulti Kejuruteraan Mekanikal — Devarajan Ramasamy — Development Of Micropump In Fuel Cell Application Using Micro Electro-Mechanical System (Mems) — 2010

ACKNOWLEDGEMENTS

For the development and production of this report, we feel a deep sense of gratitude:

- To Prof Dr. Rosli Abu Bakar – Dean, Faculty of Mechanical Engineering.
- To Mr Amiruddin Abdul Kadir – Deputy Dean, Faculty of Mechanical Engineering
- To Mr Muhammad Mat Noor – Deputy Dean Of Research of Mechanical Engineering who was also the researcher for this project.
- To all Deputy Deans and Head of Programs
- To all Lecturers, Teaching Engineers, Assistant Teaching Engineers, graduate students and all involved in this project.

ABSTRACT

DEVELOPMENT OF MICROPUMP IN FUEL CELL APPLICATION USING MICRO ELECTRO-MECHANICAL SYSTEM (MEMS) MACHINING METHOD

(Keywords: CFD, Fluid Flow, Micropump)

The need for cooling in advance thermal systems is ever in demand. The administration of such cooling will need miniaturization of the current pumping system for small scale use. A valve less pump is one of the methods to create a small microscale flowrate pump. It has intake and outlet on the same side. Advances in fluid mechanics are able to capture the working principles of such pumps and give a close approximation of the pump characteristics. The fundamental aspect that a micropump will endure is analysed from fluid mechanics analysis, is a key in the development of the model. The sizing and criteria of the pump is set based on fluid equations of mass, momentum and energy. A design is laid out by using computer aided design (CAD) based on the voltage frequency that will be applied to the piezomaterial. The movement of the material due to current will cause the fluid to move as the material will act as a diaphragm. The design is then analysed using computational fluid dynamics (CFD) from the frequency inputs and a steady flow design is simulated. The reading of the small flowrate is analysed and a proper method of designing the valve less pump is gathered.

Key researchers:

Devarajan Ramasamy

E-mail : **deva@ump.edu.my**
Tel. No. : **09-4242221**
Vote No. : **RDU 09/03/66**

ABSTRAK

PEMBANGUNAN PAM MIKRO UNTUK PENGGUNAAN SEL BAHAN API MENGGUNAKAN PEMESINAN SISTEM MIKRO ELEKTRO-MEKANIKAL (MEMS)

(Keywords: CFD, Kadar Alir Bendalir, Mikro pam)

Keperluan penyejukan dalam system thermo pada masa kini adalah sangat diperlukan. Untuk mencapai keperluan ini pengecilan system pam yang ada sekarang perlu dibuat untuk skala kecil. Pam yang tidak mempunyai injap merupakan salah satu cara untuk membawa kadar alir berskala mikro. Ia mempunyai kemasukan dan keluaran pada bahagian yang sama. Prinsip bekerja pa mini didapati daripada perkembangan dalam bidang mekanik bendalir untuk menentukan cirri-ciri pam yang berskala kecil ini. Kajian bendalair akan menentukan sejauh mana pa mini dapat bertahan dan membolehkan pembangunan model awal pam ini. Saiz dan kriteria pam diperolehi semasa penyelesaian persamaan bendalir untuk jisim, momentum dan tenaga. Rekabentuk awal dibuat dengan CAD berdasarkan frequency voltan yang akan diberi kepada bahan piezo. Bahan ini akan bertindak sebagai diafragma yang menyebabkan kadar alir bendalir semasa ia bergetar dengan frekuensi yang diberi. Rekabentuk ini kemudian dikaji dengan applikasi dinamik bendalir berkomputer daripada input frekuensi dan simulasi berterusan. Kadaralir yang rendah ini dikaji dan suatu cara kerja untuk rekabentuk pam yang tiada injap ini diperolehi.

TABLE OF CONTENTS

Page

LIST OF FIGURES

LIST OF ABBREVIATIONS

MEMS	Microelectromechanical systems
CFD	Computational fluid dynamics
DDS.	drug delivery system
CAD	Computer-aided design
SMA	Surface Mount Assembly
CRO	Cathode-ray oscilloscope
ADC	analog-to-digital converter
IC	integrated circuit

LIST OF ATTACHMENTS

CHAPTER 1

INTRODUCTION

While miniaturization is revolutionizing the world of sensors and various mechanical systems, Micro fluidics is currently one of the major areas of application of miniature devices. While many mechanical systems are now feasible on a micro scale, devices like micro pumps, miniature mixers, flow sensors, etc. are already commercially available and widely used. These micro pumps find their greatest application in chemical and biomedical also in electronic applications requiring the transport of small, accurately measured liquid quantities. When utilized in chemical applications, micro pumps are often a component of a lab-on-a-chip device. Such devices are envisioned as providing for reasonably inexpensive, possibly even disposable, means to conduct laboratory experiments.

Micro pumps can be classified into two groups: mechanical pumps with moving parts and non-mechanical pumps without moving parts. Two movement mechanisms have been employed in mechanical micro pumps: reciprocating and peristaltic movements. The actuator play very important roles in achieving the maximum flow rate and the output pressure of the pump. The maximum output pressure of a micro pump depends directly on the available force an actuator can deliver.

Research Methodology

There are many types of micro pump had been creating with many types of function. Most of these micro pumps have complex structures and high power consumption. On the contrary, piezoelectric actuation has advantages due to its relatively simple structure and lower power consumption.

One of the types of micro system is using circular piezoelectric micro pump. This study helps to improve the performance of the circular piezoelectric micro pump to choose the best size and also functional to be applied in the industry. This project also can help increase the accuracy fluid flow rate depend on the used.

Objective

i. Design a suitable size micro pump.
ii. Analysis of ideal diffuser angle.
iii. Design of piezo electrical circuit.

Scope of research

i. Initial study for micro pump application.
ii. CAD modeling of micro pump.
iii. CFD analysis for diffuser angle.
iv. Experiment setup of micro pump and circuit.

CHAPTER 2

2.0 Background

Micropumps are the essential components in the DDS. Since one of the early piezoelectric micropumps for insulin delivery was fabricated in 1978, various mechanical micropumps with different actuating principle have been developed , such as thermopneumatic , electrostatic, shape memory alloy (SMA) , electromagnetic as well as piezoelectric. The piezoelectric actuation presents its advantages of moderately pressure and displacement at simultaneously low power consumption, good reliability and energy efficiency . These features are preferred for medical application. Microsystems have the advantages of small volume, cheap cost, high precision and fast reaction time. Micro pumps are essential devices in the micro fluidic systems, which provide momentum to cause fluid flow. One recent key application of micro pumps is to provide a means to deliver insulin to many diabetic patients, thus providing an alternative to injections. Such types of micro pumps can be programmed to administer insulin at a constant rate throughout the day, thus eliminating any surges or deficits of the drug in the patient's bloodstream. The first important step towards ascertaining the reliability of a pump design is to focus on the stresses experienced by the pump during its operation.

2.1 Oscilloscope

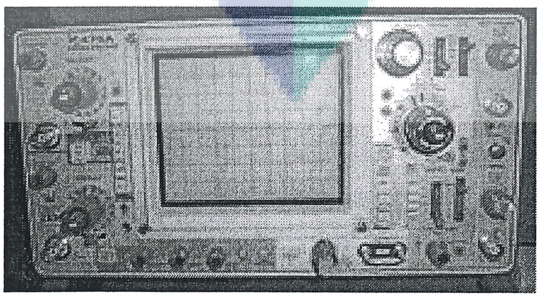

Figure 2.1 : Digital Oscilloscope

Source : http://www-ese.fnal.gov/eseproj/BTeV/BTeV_Russia/default.html

Oscilloscope is a type of electronic test instrument that allows signal voltages to be viewed, usually as a two-dimensional graph of one or more electrical potential differences (vertical axis) plotted as a function of time or of some other voltage (horizontal axis). Although an oscilloscope displays voltage on its vertical axis, any other quantity that can be converted to a voltage can be displayed as well. In most instances, oscilloscopes show events that repeat with either no change or change slowly.

Oscilloscopes are used when it is desired to observe the exact wave shape of an electrical signal. In addition to the amplitude of the signal, an oscilloscope can show distortion and measure frequency, time between two events (such as pulse width or pulse rise time), and relative timing of two related signals. Oscilloscopes are used in the sciences, medicine, engineering, telecommunications, and industry. General-purpose instruments are used for maintenance of electronic equipment and laboratory work. Special-purpose oscilloscopes may be used for such purposes as analyzing an automotive ignition system, or to display the waveform of the heartbeat as an electrocardiogram.

Originally all oscilloscopes used cathode ray tubes as their display element and linear amplifiers for signal processing, but modern oscilloscopes can have LCD or LED screens, fast analog-to-digital converters and digital signal processors and some oscilloscopes used storage CRTs to display single events for a limited time. Oscilloscope peripheral modules for general purpose laptop or desktop personal computers use the computer's display, and can convert them into useful and flexible test instruments.

Oscilloscopes generally have a checklist. The basic measure of virtue is the bandwidth of its vertical amplifiers. Typical scopes for general purpose use should have a bandwidth of at least 100 MHz, although much lower bandwidths are acceptable for audio-frequency applications. A useful sweep range is from one second to 100 nanoseconds, with triggering and delayed sweep.

2.1.1 Oscilloscope Basic Functional

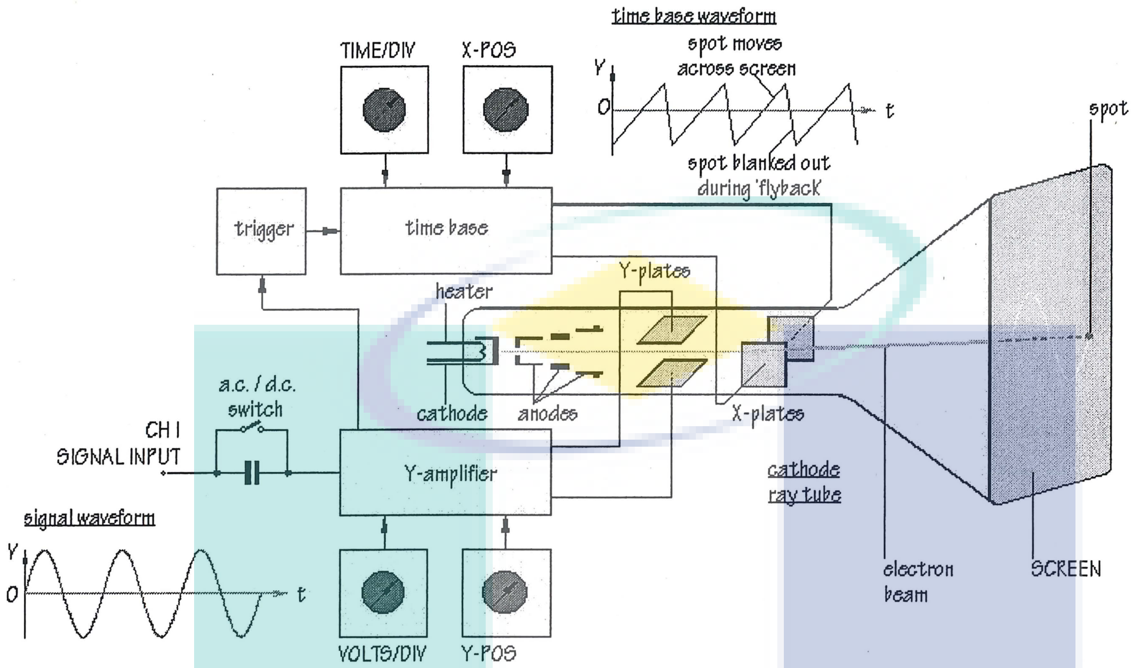

Figure 2.2 : Oscilloscope Basic Diagram

Source : http://www.tpub.com/content/neets/14188/css/14188_189.htm

Like a television screen, the screen of an oscilloscope consists of a **cathode ray tube**. Although the size and shape are different, the operating principle is the same. Inside the tube is a vacuum. The electron beam emitted by the heated cathode at the rear end of the tube is accelerated and focused by one or more anodes, and strikes the front of the tube, producing a bright spot on the phosphorescent screen.

The electron beam is bent, or deflected, by voltages applied to two sets of plates fixed in the tube. The horizontal deflection plates or **X-plates** produce side to side movement. As you can see, they are linked to a system block called the time base. This produces a saw tooth waveform. During the rising phase of the saw tooth, the spot is driven at a uniform rate from left to right across the front of the screen. During the falling phase, the electron beam returns rapidly from right or left, but the spot is 'blanked out' so that nothing appears on the screen.

In this way, the time base generates the X-axis of the *V/t* graph.

The slope of the rising phase varies with the frequency of the saw tooth and can be adjusted, using the TIME/DIV control, to change the scale of the X-axis. Dividing the oscilloscope screen into squares allows the horizontal scale to be expressed in seconds, milliseconds or microseconds per division (s/DIV, ms/DIV, and μs/DIV). Alternatively, if the squares are 1 cm apart, the scale may be given as s/cm, ms/cm or μs/cm.

The signal to be displayed is connected to the **input**. The AC/DC switch is usually kept in the DC position (switch closed) so that there is a direct connection to the **Y-amplifier**. In the AC position (switch open) a capacitor is placed in the signal path. As will be explained in Chapter 5, the capacitor blocks DC signals but allows AC signals to pass.

The Y-amplifier is linked in turn to a pair of **Y-plates** so that it provides the Y-axis of the *V*/*t* graph. The overall gain of the Y-amplifier can be adjusted, using the VOLTS/DIV control, so that the resulting display is either too small or too large, but fits the screen and can be seen clearly. The vertical scale is usually given in V/DIV or mV/DIV.

The **trigger** circuit is used to delay the time base waveform so that the same section of the input signal is displayed on the screen each time the spot moves across. The effect of this is to give a stable picture on the oscilloscope screen, making it easier to measure and interpret the signal.

Changing the scales of the X-axis and Y-axis allows many different signals to be displayed. Sometimes, it is also useful to be able to change the *positions* of the axes. This is possible using the X-POS and **Y-POS** controls. For example, with no signal applied, the normal trace is a straight line across the centre of the screen. Adjusting Y-POS allows the zero level on the Y-axis to be changed, moving the whole trace up or down on the screen to give an effective display of signals like pulse waveforms which do not alternate between positive and negative values.

2.1.2 Types of Oscilloscope

Cathode-ray oscilloscope (CRO) The earliest and simplest type of oscilloscope consisted of a cathode ray tube, a vertical amplifier, a time base, a horizontal amplifier and a power supply. These are now called 'analog' scopes. The cathode ray tube is an evacuated glass envelope, similar to that in a black-and-white television set, with its flat face covered in a fluorescent material (the phosphor). The screen is typically less than 20 cm in diameter.

The extra features that this system provides include:

- on-screen display of amplifier and time base settings;
- voltage cursors - adjustable horizontal lines with voltage display;
- time cursors - adjustable vertical lines with time display;
- On-screen menus for trigger settings and other functions.

Dual-beam oscilloscope was a type of oscilloscope once used to compare one signal with another. There were two beams produced in a special type of CRT. Unlike an ordinary "dual-trace" oscilloscope (which time-shared a single electron beam, thus losing about 50% of each signal), a dual-beam oscilloscope simultaneously produced two separate electron beams, capturing the entirety of both signals. One type (Cossor, UK) had a beam-splitter plate in its CRT, and single-ended vertical deflection following the splitter.

Analog storage oscilloscope is an extra feature available on some analog scopes; they used direct-view storage CRTs. Storage allows the trace pattern that normally decays in a fraction of a second to remain on the screen for several minutes or longer. An electrical circuit can then be deliberately activated to store and erase the trace on the screen. The storage is accomplished using the principle of secondary emission.

Analog Sampling Oscilloscope achieves their large bandwidths by not taking the entire signal at a time. Instead, only a sample of the signal is taken. The samples are then assembled to create the waveform. This method can only work for repetitive signals, not transient events. The idea of sampling can be thought of as a stroboscopic technique. When using a strobe light, only pieces of the motion are seen, but when enough of these images are taken, the overall motion can be captured

Digital oscilloscopes digital devices employ binary numbers which correspond to samples of the voltage. In the case of digital oscilloscopes, an analog-to-digital converter (ADC) is used to change the measured voltages into digital information. Waveforms are taken as a series of samples. The samples are stored, accumulating until enough are taken in order to describe the waveform, which are then reassembled for display. Digital technology allows the information to be displayed with brightness, clarity, and stability. There are, however, limitations as with the performance of any oscilloscope. The highest frequency at which the oscilloscope can operate is determined by the analog bandwidth of the front-end components of the instrument and the sampling rate. Digital oscilloscopes can be classified into three primary categories:

1. Digital storage oscilloscopes.

2. Digital phosphor oscilloscopes.

3. Digital sampling oscilloscopes

Mixed-signal oscilloscope (or MSO) has two kinds of inputs, a small number (typically two or four) of analog channels, and a larger number (typically sixteen) of digital channels. These measurements are acquired with a single time base, they are viewed on a single display, and any combination of these signals can be used to trigger the oscilloscope. An MSO combines all the measurement capabilities and the use model of a Digital Storage Oscilloscope (DSO) with some of the measurement capabilities of a logic analyzer. MSOs typically lack the advanced digital measurement capabilities and the large number of digital acquisition channels of full-fledged logic analyzers, but they are also much less complex to use. Typical mixed-signal measurement uses include the characterization and debugging of hybrid analog/digital circuits like: embedded systems, Analog-to-digital converters (ADCs), Digital-to-analog converters (DACs), and control systems.

Handheld oscilloscopes (also called scopemeters) are useful for many test and field service applications. Today, a hand held oscilloscope is usually a digital sampling oscilloscope, using a liquid crystal display. Typically, a hand held oscilloscope has two analog input channels, but four input channel versions are also available. Some instruments combine the functions of a digital multimeter with the oscilloscope. Usually lightweight with good accuracy.

PC-based oscilloscopes (PCO) is emerging that consists of a specialized signal acquisition board (which can be an external USB or Parallel port device, or an internal add-on PCI or ISA card). The hardware itself usually consists of an electrical interface providing isolation and automatic gain controls, several high-speed analog-to-digital converters and some buffer memory, or even on-board Digital Signal Processor (DSPs). Depending on the exact hardware configuration, the hardware could be best described as a digitizer, a data logger or as a part of a specialized automatic control system.

2.2 Piezoelectric

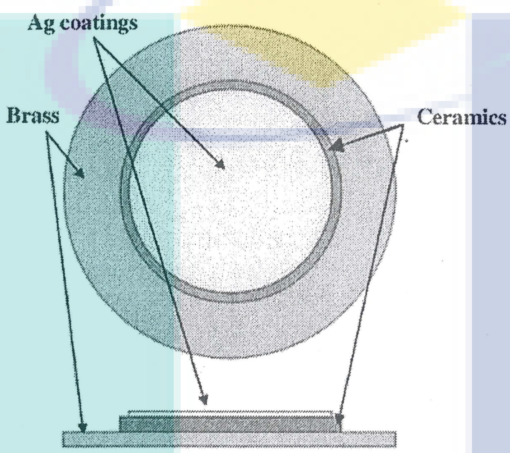

Figure 2.3: Piezoelectric

Source : http://www.physikinstrumente.com/tutorial/index.htm

Piezoelectricity is the ability of some materials (notably crystals and certain ceramics, including bone) to generate an electric field or electric potential in response to applied mechanical stress. The effect is closely related to a change of polarization density within the material's volume. If the material is not short-circuited, the applied stress induces a voltage across the material. The word is derived from the Greek *piezo* or *piezein*, which means to squeeze or press.

The piezoelectric effect is reversible in that materials exhibiting the *direct piezoelectric effect* (the production of an electric potential when stress is applied) also exhibit the *reverse piezoelectric effect* (the production of stress and/or strain when an electric field is applied). For example, lead zirconate titanate crystals will exhibit a maximum shape change of about 0.1% of the original dimension.(O. Ohnishi, H. Kishie, A. Iwamoto, Y. Sasaki, T. Zaitsu, T. Inoue, Piezoelectric ceramic transformer operating in thickness extensional vibration mode for power supply, in: Proc. IEEE Ultrason. Symp., vol. 1, 1992, pp. 483–488.)

The effect finds useful applications such as the production and detection of sound, generation of high voltages, electronic frequency generation, microbalances, and ultra fine focusing of optical assemblies.

2.2.1 Materials and Design Piezo

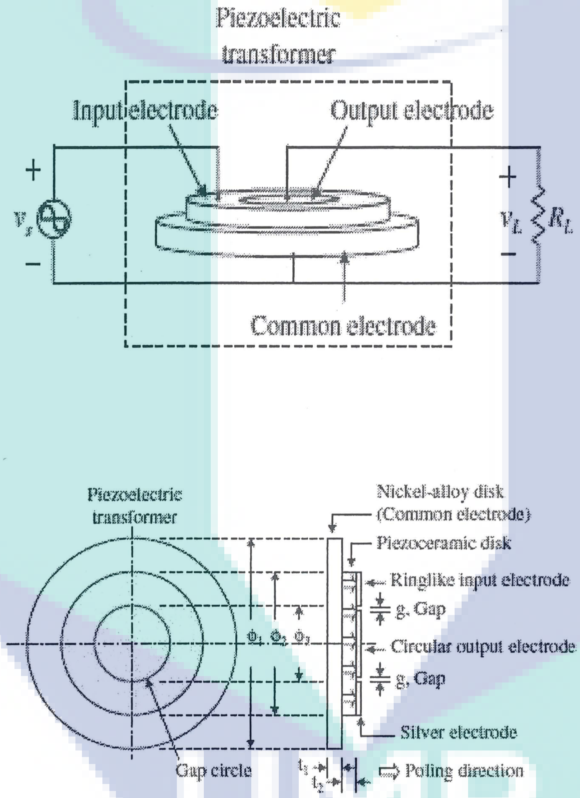

Figure 2.4 : Piezo basic design

Source : http://www.answers.com/topic/piezoelectricity

Piezoelectric buzzer includes a nickel-alloy disc, and a piezoceramic disc covered with a silver electrode and a gap circle on the silver electrode are needed to build a single-input-and-single-output thin disc PT. All of the nickel-alloy disc, the piezoceramic disc and the gap circle are concentric with each other. The piezoceramic disc has a poling direction in the thickness direction. The thin disc PT has three electrodes, including a ring-shaped input electrode, a circular-shaped output electrode and a common electrode. The common electrode is implemented by the nickelalloy disc, and the input and output electrodes are obtained from the silver electrode with a gap circle. An AC voltage vs is connected to the input electrode, and a load resistor RL is connected to the output electrode.

In principles of the thin disc PT, an input part of the thin disc PT is operated by converse piezoelectric effect so as to convert the electrical energy to the mechanical energy, and an output part of the thin disc PT is operated by direct piezoelectric effect so as to convert the mechanical energy to the electrical energy. Compressive or extensive deformation of a piezoelectric body happens due to the converse piezoelectric effect when the piezoelectric body is electrically energized by a DC voltage. Also, a DC voltage is induced at both terminals of the piezoelectric body due to direct piezoelectric effect when the piezoelectric body is mechanically energized by a compressive or extensive force.

Piezoelectric equations for deriving electromechanical conversion principles of any type of piezoelectric bodies are expressed as follows:

$$\{T\} = [c]\{S\} - [e]\{E\} \tag{1}$$

$$\{D\} = [e]^T\{S\} + [\varepsilon]\{E\} \tag{2}$$

where {T} is the stress vector, {S} is the strain vector, {E} is the electric field vector, {D} is the electric flux density vector, [c] is the elastic constant matrix, [e] is the piezoelectric constant matrix, [e] is the dielectric constant matrix, and [e]T is the transposition matrix of [e].

For the buzzer, the bending vibration mode occurs in the axissymmetrical piezoceramic disc shown and determined according to the following equation:

$$\frac{\partial^2 uT}{\partial r^2} + \frac{1}{r}\frac{\partial uT}{\partial r} = \frac{1}{c^2}\frac{\partial^2 uT}{\partial t^2} \tag{3}$$

Where uT is the instant vibration amplitude, c is the acoustic velocity, and r is the radius from the center of the piezoceramic disc. Then, substituting boundary conditions, including $\lim_{r\to 0uT}(r,t)$= bounded and uT(Φ_2 / 2,t) into Equation (3) yields:

$$\sum_{m=1}^{\infty} A_m J_0(\xi r) e^{jc\xi} m^1 \quad (4)$$

Where,

$$\xi_m = 2\alpha_m^0 / \Phi_2 \quad (5)$$

$$C^2 = T/\rho \quad (6)$$

2.3 Diffuser / Nozzle

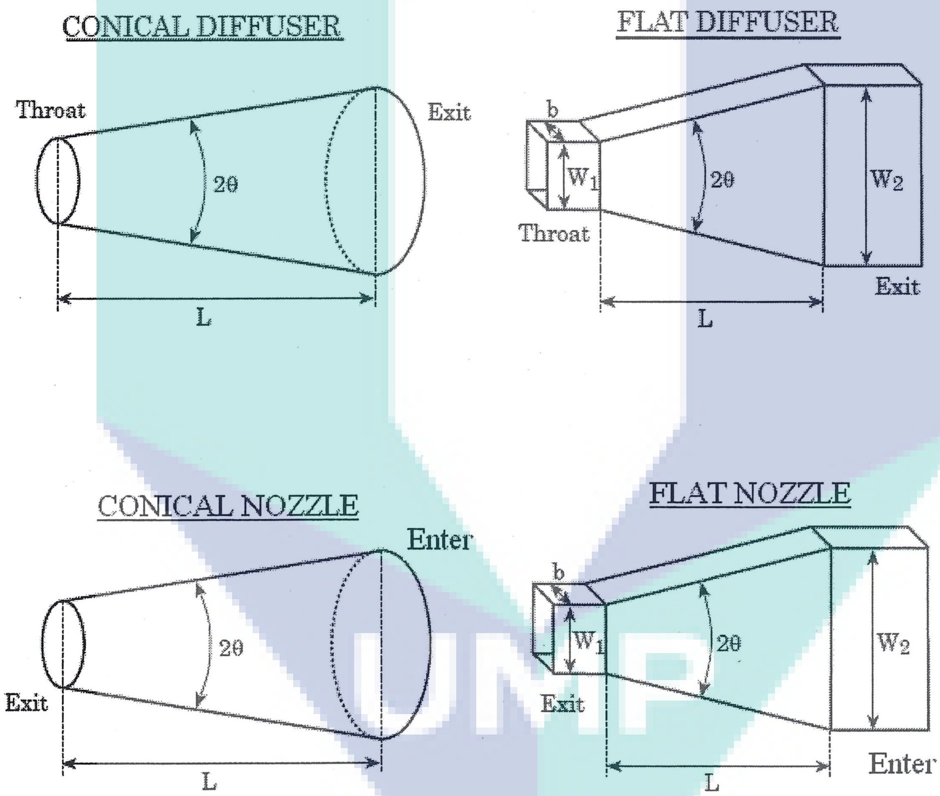

Figure 2.5 : Conical and Flat Diffuser and Nozzle.
Source : (T. Gerlach, M. Schuenemann, and H. Wurmus, "A new micropump principle of the reciprocating type using pyramidic micro flow channels as passive valves," *Journal of Micromechanics and Microengineering*, vol. 5, pp. 199-201, 1995)

In the diffuser pump diffuser elements are used as flow directing elements. Wear and fatigue are therefore eliminated since the diffuser pump has no moving parts and the risk of valve clogging is also reduced. The diffuser pump is a positive displacement pump in the sense that it has a moving boundary which forces the fluid along by volume changes. As other positive displacement pumps it delivers a periodic flow. The pump principle has been shown to work for different.

The diffuser, a flow channel with gradually expanding cross-section, is the key element in the valve-less diffuser pump. Used in the opposite direction with converging cross-section it is called a nozzle. Diffusers usually have circular or rectangular cross-sections as illustrated in Figure 2.5. They are called conical and flat-walled diffusers, respectively. Both diffusers and nozzles are common devices in macroscopic internal flow systems.

The function of the diffuser is to transform kinetic energy, e.g. flow velocity, to potential energy, e.g. pressure. The type of flow in a diffuser can be exemplified by a 'stability map', as shown in Figure 2.6. The map shows that depending on the diffuser geometry, the diffuser works in four different regions. In the *no stall* region the flow is steady viscous with no separation at the diffuser walls and moderately good performance. In the *transitory steady stall* region the flow is unsteady and it is in this region we have the minimum pressure loss. In the *bistable steady region* a steady bistable stall can flip-flop from one part of the diffuser wall to another and the performance is poor. In the *jet flow* region the flow separates almost completely from
the diffuser walls and passes through the diffuser at nearly constant cross-sectional area making its performance extremely poor .

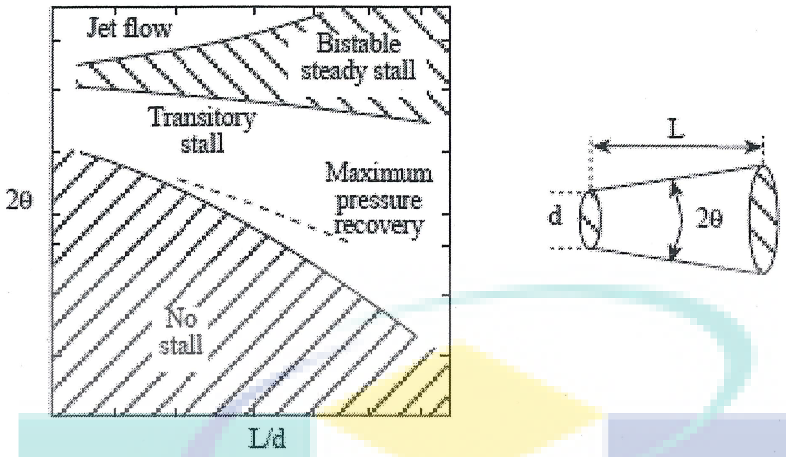

Figure 2.6 : A stability map of a diffuser used to design a diffuser geometry with minimal pressure loss coefficient.

Source : (FM White, FIuid ***Mechanics,*** McGraw-Hill, New York, 1986, pp 332-339 and 345-371)

Basic equation for Diffuser and Nozzle:

$$\Delta P_{diffuser} = \xi_{diffuser} \cdot \frac{1}{2} \rho \pi^2_{diffuser} \quad (1)$$

$$\Delta P_{nozzle} = \xi_{nozzle} \cdot \frac{1}{2} \rho \pi^2_{nozzle} \quad (2)$$

$$\eta = \frac{\xi_{nozzle}}{\xi_{diffuser}} \quad (3)$$

$$V_c = V_0 \sin 2\pi f t \quad (4)$$

$$V_0 = K_v x_0 \quad (5)$$

$$\Phi = \frac{K_v x_0 \omega}{\pi} \left(\frac{\eta^{\frac{1}{2}} - 1}{\eta^{\frac{1}{2}} + 1} \right) \quad (6)$$

During the supply mode the chamber volume increases, dV,/df > 0, which gives a net flow into the chamber with the inlet element acting as a diffuser and the outlet element acting as a nozzle, see Figure 2.7 This gives inlet and outlet flows of $\Phi_1 = \Phi_d = C/\ (\xi_d)^{\frac{1}{2}}$ and $\Phi_0 = -\Phi_n = -C/\ (\xi_n)^{\frac{1}{2}}$ This yields a net chamber flow of $\Phi_1 - \Phi_0 = C\ (\frac{1}{(\xi_d)^{\frac{1}{2}}} + \frac{1}{(\xi_n)^{\frac{1}{2}}}) = V_x\ \omega \cos \omega t$ which gives $C = V_x\ \omega \cos \omega t\ /\ (\frac{1}{(\xi_d)^{\frac{1}{2}}} + \frac{1}{(\xi_n)^{\frac{1}{2}}})$ the supply mode outlet flow is $\Phi_0 = -\Phi_n = -C/\ (\xi_n)^{\frac{1}{2}}$ which with the expression for C yields $\Phi_1 = -V_x\ \omega \cos \omega t\ /\ [\ 1 + (\xi_n/\xi_d)^{1/2}\ ]$.

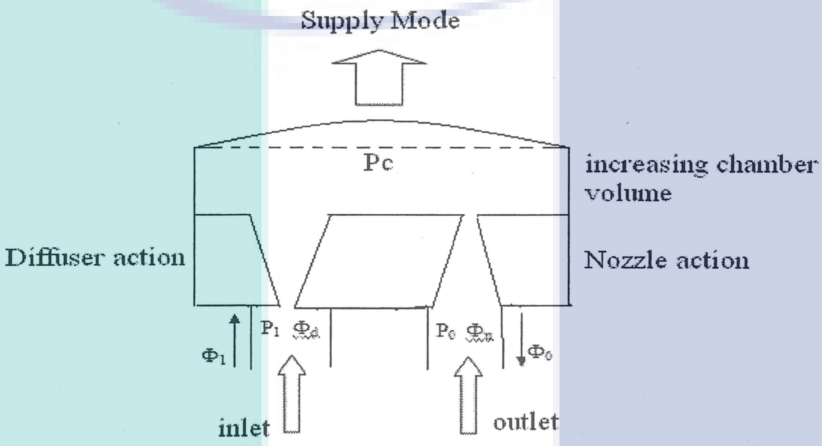

Figure 2.7 : Supply Mode

Source : http://www.sciencedirect.com/science?_ob=ArticleURL&_udi=B6THG-486G7X8-2&_user=2809665&790979d8d9d27555a61bd0239da30ac#toc2

During the pump mode the chamber volume decreases, ***dV/df* <O,** which gives a net flow out of the chamber with the inlet element acting as a nozzle and the outlet element acting as a diffuser, see Figure 2.8 This gives inlet and outlet flows of $\Phi_1 = -\Phi_n = -C/\ (\xi_n)^{\frac{1}{2}}$ and $\Phi_0 = \Phi_d = C/\ (\xi_d)^{\frac{1}{2}}$ similar calculations as for the supply mode yield a pump-mode outlet flow of $\Phi_p = -V_n\ \omega \cos \omega t\ /\ [\ 1 + (\xi_d/\xi_n)^{1/2}\ ]$. (T. Gerlach and H. Wurmus, "Working principle and performance of the dynamic micropump," *Sensor and Actuators*, vol. A50, pp. 135-140, 1995.)

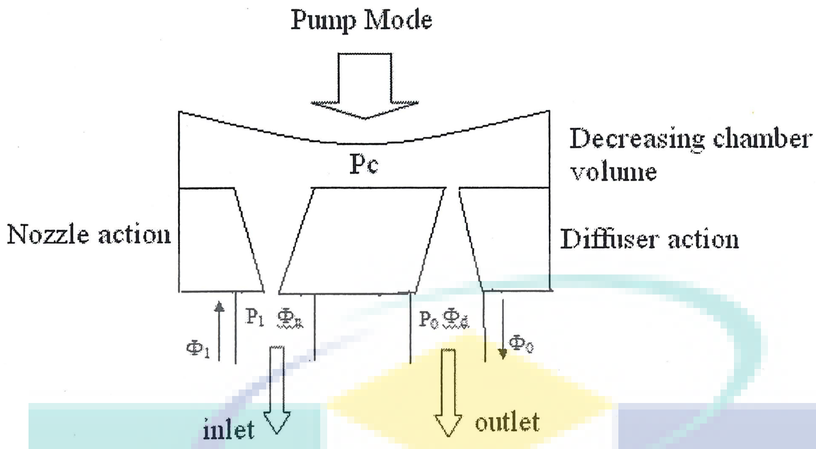

Figure 2.8: Pump Mode

Source : http://www.sciencedirect.com/science?_ob=ArticleURL&_udi=B6THG-486G7X8-2&_user=2809665&790979d8d9d27555a61bd0239da30ac#toc2

2.4 Circuit 555 timer IC

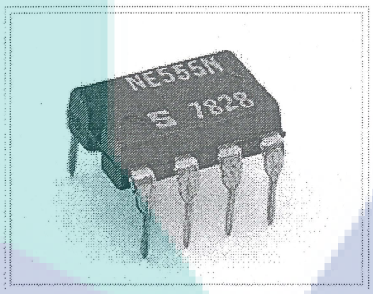

Figure 2.9 : NE 555 IC

Source : http://my.mouser.com/ProductDetail/Texas-Instruments/NE555P/

The **555 Timer IC** is an integrated circuit (chip) implementing a variety of timer and multivibrator applications. The IC was designed by Hans R. Camenzind in 1970 and brought to market in 1971 by Signetics (later acquired by Philips). The original name was the SE555 (metal can)/**NE555** (plastic DIP) and the part was described as "The IC Time Machine".[It has been claimed that the 555 gets its name from the three 5 kΩ resistors used in typical early implementations, but Hans Camenzind has stated that the number was arbitrary.

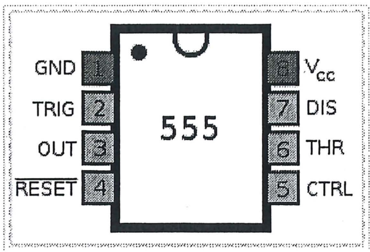

Figure 2.10 : NE555 IC diagram

Source : http://my.mouser.com/ProductDetail/Texas-Instruments/NE555P/spec/

The connection of the pins is as follows:

Nr.	**Name**	**Purpose**
1	GND	Ground, low level (0 V)
2	TRIG	A short pulse high-to-low on the trigger starts the timer
3	OUT	During a timing interval, the output stays at $+V_{CC}$
4	RESET	A timing interval can be interrupted by applying a reset pulse to low (0 V)
5	CTRL	Control voltage allows access to the internal voltage divider (2/3 V_{CC})
6	THR	The threshold at which the interval ends (it ends if the voltage at THR is at least 2/3 V_{CC})
7	DIS	Connected to a capacitor whose discharge time will influence the timing interval
8	$V+$, V_{CC}	The positive supply voltage which must be between 3 and 15 V

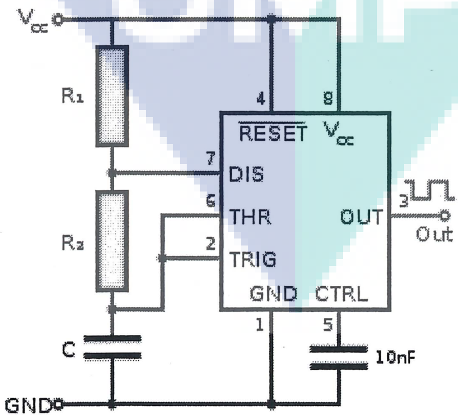

Figure 2.11 : Astable Mode Circuit For NE555 IC

Source : http://en.wikipedia.org/wiki/555_timer_IC

In astable mode, the '555 timer ' puts out a continuous stream of rectangular pulses having a specified frequency. Resistor R_1 is connected between V_{CC} and the discharge pin (pin 7) and another resistor (R_2) is connected between the discharge pin (pin 7), and the trigger (pin 2) and threshold (pin 6) pins that share a common node. Hence the capacitor is charged through R_1 and R_2, and discharged only through R_2, since pin 7 has low impedance to ground during output low intervals of the cycle, therefore discharging the capacitor.

In the astable mode, the frequency of the pulse stream depends on the values of R_1, R_2 and C: (van Roon Chapter: "Astable operation.").

$$f = \frac{1}{\ln(2).C.(R_1+2R_2)} \quad (1)$$

the high time from each pulse is given by

$$high = \ln(2).(R_1 + R_2).C \quad (2)$$

and the low time from each pulse is given by

$$low = \ln(2).R_2.C \quad (3)$$

CHAPTER 3

Paper 1

1. **R.Devarajan**, S.Mahendran, Zainal Ambri Abdul Karim, T.Nagarajan, "Development of Valve Less Micropump Preliminary Characteristics from Fluid Flow",11th Electronics Materials And Packaging Conference EMAP, December 1- 3, 2009 Universiti Sains Malaysia, Pulau Pinang, 2009.

Development of Valve Less Micropump Preliminary Characteristics from Fluid Flow

R.Devarajan[1], S. Mahendran[1], Zainal Ambri Abdul Karim[2], T.Nagarajan[2]
[1]Faculty of Mechanical Engineering, Universiti Malaysia Pahang, 26300 Kuantan, Pahang, Malaysia.
Phone: +609-5492223, Fax: +609-5492244. Email: deva@ump.edu.my

[2]Department of Mechanical Engineering,Universiti Teknologi PETRONAS, Bandar Seri Iskandar, 31750 Tronoh, Perak Darul Ridzuan, Malaysia. Phone: +605-3687028, Fax:+605-3656461
Email: nagarajan_t@petronas.com.my , ambri@petronas.com.my

ABSTRACT— THE NEED FOR COOLING IN ADVANCE THERMAL SYSTEMS IS EVER IN DEMAND. THE ADMINISTRATION OF SUCH COOLING WILL NEED MINIATURIZATION OF THE CURRENT PUMPING SYSTEM FOR SMALL SCALE USE. A VALVE LESS PUMP IS ONE OF THE METHODS TO CREATE A SMALL MICROSCALE FLOWRATE PUMP. IT HAS INTAKE AND OUTLET ON THE SAME SIDE. ADVANCES IN FLUID MECHANICS ARE ABLE TO CAPTURE THE WORKING PRINCIPLES OF SUCH PUMPS AND GIVE A CLOSE APPROXIMATION OF THE PUMP CHARACTERISTICS. THE FUNDAMENTAL ASPECT THAT A MICROPUMP WILL ENDURE IS ANALYSED FROM FLUID MECHANICS ANALYSIS, IS A KEY IN THE DEVELOPMENT OF THE MODEL. THE SIZING AND CRITERIA OF THE PUMP IS SET BASED ON FLUID EQUATIONS OF MASS, MOMENTUM AND ENERGY. A DESIGN IS LAID OUT BY USING COMPUTER AIDED DESIGN (CAD) BASED ON THE VOLTAGE FREQUENCY THAT WILL BE APPLIED TO THE PIEZOMATERIAL. THE MOVEMENT OF THE MATERIAL DUE TO CURRENT WILL CAUSE THE FLUID TO MOVE AS THE MATERIAL WILL ACT AS A DIAPHRAGM. THE DESIGN IS THEN ANALYSED USING COMPUTATIONAL FLUID DYNAMICS (CFD) FROM THE FREQUENCY INPUTS AND A STEADY FLOW DESIGN IS SIMULATED. THE READING OF THE SMALL FLOWRATE IS ANALYSED AND A PROPER METHOD OF DESIGNING THE VALVE LESS PUMP IS GATHERED.

***Key Words*—CFD, Fluid Flow, Micropump.**

Introduction

As microelectronics is expanding with wide demands of computing, the need to manage the thermal aspects of systems is playing a critical role in the packaging industries. With high power density levels, computer mainframes, telecommunication equipments, supercomputers and high powered systems will increasingly require improved cooling that is not possible that traditional air-cooling or direct immersion cooling technologies. As such a novel cooling method with improve pumping performance is crucial to in facing the growing need of the electronic markets.

Micropumps have been developed by using several actuation methods, such as electromagnetic [1], piezoelectric [2],[3],[4],[5],[6],[7],[8], shape memory alloy [9], electrostatic[10],[11], and thermo-pneumatic [12] devices. Most of these micropumps have complex structures and high power consumption. On the contrary, piezoelectric actuation has advantages due to its relatively simple structure and lower power consumption.

In this study, a new type of thin, compact, and light weighed diaphragm micropump will be developed to actuate liquid by the vibration of a diaphragm. The amplitude of vibration by a piezoelectric device produces an oscillating flow and alters the chamber volume by the curvature change of a diaphragm. This enables the pump to function to transfer fluids such as water or air.

A valve less pump consists of two fluid flow rectifying diffuser/nozzle elements which are connected to the inlet and outlet of a pump chamber with a flexible diaphragm. Stemme, [2] proposed the first prototype of valve less pump consisting of a circular cylindrical volume where the top side had a thin brass diaphragm to which a piezoelectric disc was fixed. Its flow rate was 15.6 ml/min. Olssen et al, [3,13] investigated the flow-directing properties of several diffuser elements with different lengths and opening angles for valve less micropumps. Numerical simulations were done by using the Computational Fluid Dynamics program ANSYS/Flotran. They found that a commercial micropump with a valve can be developed with central actuating as in Fig, 1. The drawback is the manufacture and installation of the valve.

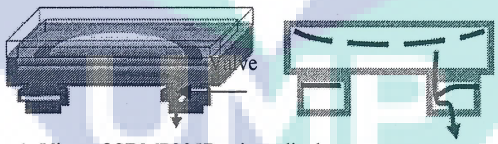

Fig. 1 View of SDMP305D micro-diaphragm pump

The aim of the study is to obtain a simple three dimensional model of the micropump enhanced without a valve using computer aided design (CAD). The model will be tested using CFD to observe the operation of the prototype.

THEORY

In Fig. 2, a new micro-diaphragm pump with piezoelectric effect has been designed to actuate the working fluid by the vibration of a diaphragm with one-side sector-shaped piezoelectric device. The vibration amplitude of the piezoelectric device produces an oscillating flow and alters the chamber volume by the curvature change of a diaphragm.

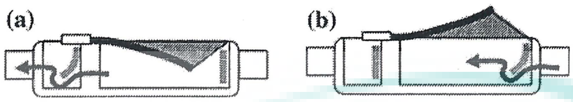

Fig.2 Working principles of a single acting micropump

When the actuator moves downwards to decrease chamber volume shown in Fig. 2a, the outflow will be in one direction by moving from a inlet diffuser to an outlet diffuser. When the actuator moves upwards to increase chamber volume shown in Fig. 2b, the fluid flowing into the pump will be in the chamber through the diverged cone, while the fluid outlet will be from the converged cone of the pump as in Fig. 3.

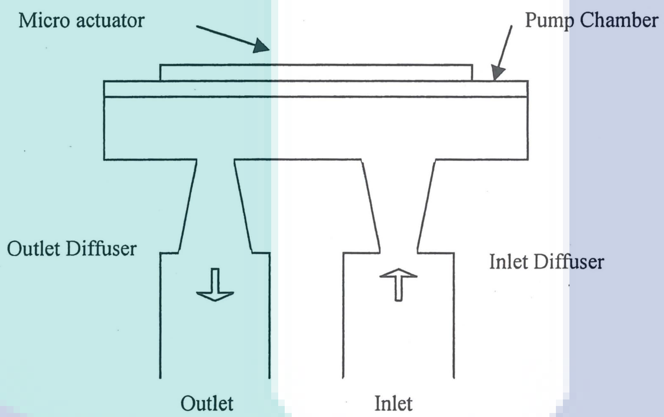

Fig. 3 Working principle of valve less micropump

In addition, the actuating force can be enforced by its harmonic resonance of the working fluid with the vibration of a rectangular piezoelectric device, diaphragm, and two cones in the pump chamber. The design of the cones is important in terms of fluid moving into the inlet and going out. The structure of nozzle/diffuser cone is shown in Fig. 4.

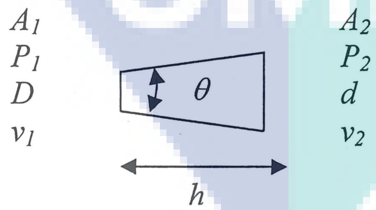

Fig. 4 Cone dimensions

From fluid mechanics it is known that, the dynamic resistance is minimum at the range of $\theta = 5°$, and the dynamic resistance is maximum when $\theta = 7°$. To start the analysis the minimum angle is used. The flow equation of clearance and pressure distribution of nozzle is given by

$$p = p_1 - \Delta p \frac{\left(\frac{D}{h}\right)^2 - 1}{\left(\frac{D}{d}\right)^2 - 1} \qquad (1)$$

And pressure distribution of cone can be expressed as

$$p = p_1 - \Delta p \frac{1 - \left(\frac{d}{h}\right)^2}{1 - \left(\frac{d}{D}\right)^2} \qquad (2)$$

Where h, being the cross sectional diameter of the cone. The flow equation of the cone is given by the Bernoulli equation as,

$$\frac{p_1}{\rho g} + \frac{v_1^2}{2g} = \frac{v_2^2}{2g} + \sum \zeta \frac{v_2^2}{2g} \qquad (3)$$

Where,

$$v_1 = v_2 \left(\frac{d}{D}\right)^2$$

$$\Delta p = p_1 - p_2$$

$$p_2 = 0$$

and,

$$v_2 = \frac{1}{\sqrt{1 + \sum \zeta - \left(\frac{d}{D}\right)^4}} \sqrt{\frac{2p_1}{\rho}}$$

(4)

Why, $\theta = 5°$ and pipe losses estimated at, $\zeta = 0.0045$, the flow rate Q can be expressed by,

$$Q = v_2 A_2 = \frac{\pi d^2}{4} \frac{1}{\sqrt{1 + \sum \zeta - \left(\frac{d}{D}\right)^4}} \sqrt{\frac{2p_1}{\rho}} \qquad (5)$$

Based on the boundary equation above and previous research of Ma et al, [14] the opening of the converged cone is set at d = 0.6 mm, and flowrate targeted to 0.6 *ml/s*. With the two boundaries predetermined a simulation was targeted by using a CFD tool. This is because the boundary condition is important to represent the flow in the mixer for CFD analysis to begin. The CFD software utilizes the Navier Stokes equations to solve the flow behavior.

$$\frac{\partial \rho}{\partial t}+\frac{\partial}{\partial x_k}(\rho u_k)=0 \qquad (1)$$

$$\frac{\partial \rho u_i}{\partial y}+\frac{\partial}{\partial x_k}(\rho u_i u_k-\tau_{ik})+\frac{\partial P}{\partial x_i}=S_i \qquad (2)$$

$$\frac{\partial(\rho E)}{\partial y}+\frac{\partial}{\partial x_k}((\rho E+P)u_k+q_k-\tau_{ik}u_i)=S_k u_k+Q_H \qquad (3)$$

Where u is the fluid velocity, ρ is the fluid density, S_i is a mass-distributed external force per unit mass, E is the total energy per unit mass, Q_H is a heat source per unit volume, τ_{ik} is the viscous shear stress tensor and q_i is the diffusive heat flux.

The preliminary model is done as shown in Fig. 5 with both cones attached to form the micropump. A moving wall was targeted to oscillate as per the piezomaterial frequency and two outlets, one being an input and the other being an output is modeled in CFD.

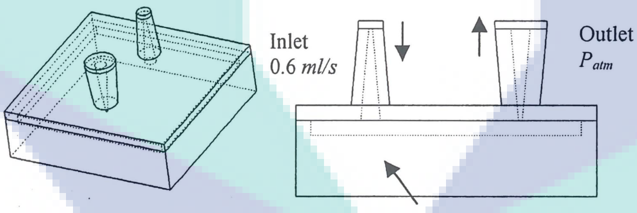

Fig. 5 Preliminary Design

RESULTS

From the software, a basic mesh is obtained showing the path that will be taken by the fluid into the micropump system. Fig. 6 shows the grid distribution in the small cavity. The spacing is done automatically by the software for the preliminary analysis to show the system functionality.

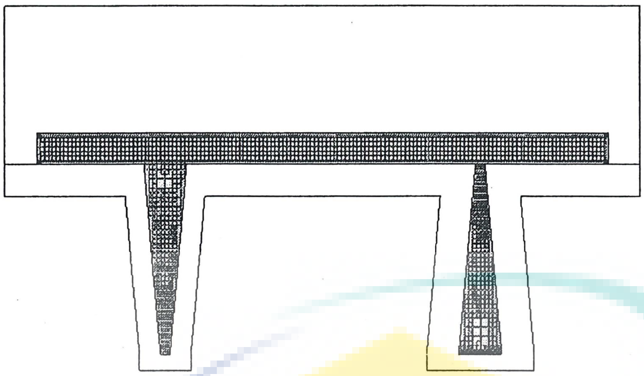

Fig. 6 Grid Spacing

The results obtained for pressure and velocity show that the pump cavity can deliver the flow as per calculations. Fig. 7 and 8 shows the respective simulation. There seem to be a small pressure buildup as the flow is moving from the inlet and exiting the outlet. The amount is small about 18 Pa. This creates very little pressure drop to the system and is seen as an advantage to the design.

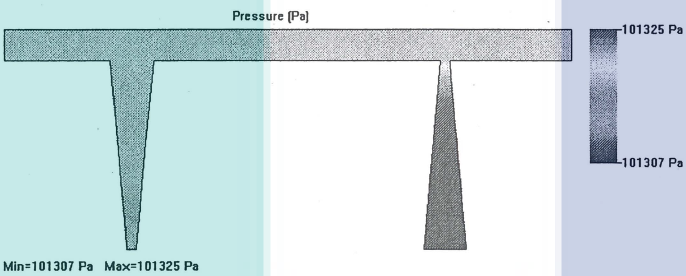

Fig. 7 Pressure Readings

In the velocity plot the converged section shows an increase in velocity. This relates to Bernoulli equation where the higher pressure region (inlet) creates a lower velocity and the lower pressure region (converged cone) create higher velocity.

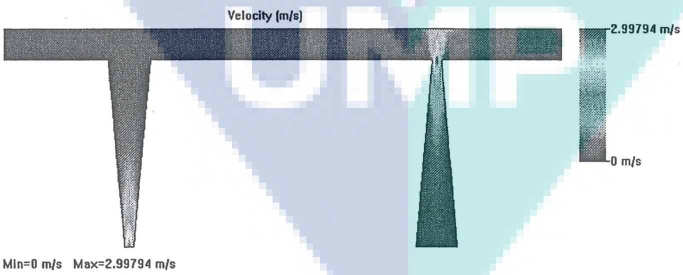

Fig. 8 Velocity Readings

Due to the velocity movement, the flow seems to accumulate more in the inlet cone, in the converging section. As seen in Fig. 9, the region may cause some fluids with particles to clog the inlet. Small foreign objects will also cause this inlet to be clogged if the flow is too fast. A fillet may help in the future design.

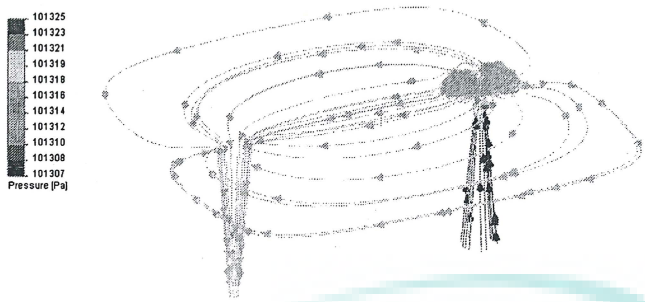

Fig. 9 Trajectories of the Flow Moving in the Pump

The other parameters that requires further investigation is on the wall, to ascertain the behavior when piezomaterial is used. The current CFD software used can only enable pressure plots and fluid flow. Hence, more elaborate models will be required to represent the wall as moving per frequency of the model.

Conclusion

The model presented in this paper is under the development stage and many unknowns still have to be finalized to obtain to the final model. The fluid flow equations from fundamental may help, but a CFD approach enables visualization with fluid properties at the micro flow level. The second challenge would be to develop the required methods to find more accurate flow speed and an experimental design will be required to lead to a solution.

ACKNOWLEDGMENT

R.Devarajan would like to thank University Malaysia Pahang for sponsor and financial support for the paper

REFERENCES

[1] Bo¨hm S, Olthuis W, Bergveld P (1999). A plastic micropump constructed with conventional techniques and materials. Sens Actuators A77:223–228.

[2] Stemme E, Stemme G (1993). A valveless diffuser/nozzle-based fluid pump. Sens Actuators A39:159–167.

[3] Olsson A, Enoksson P, Stemme G, Stemme E (1995). A valve-less planar pump in silicon. In: The 8th international conference on solid-state sensors and actuators, vol 2, pp 291–294.

[4] Koch M, Harris N, Evans AGR, White NM, Brunnschweiler A (1998). A novel micromachined pump based on thick-film piezoelectric actuation. Sens Actuators A70:98–103.

[5] Saggere L, Hagood NW, Roberts DC, Li HQ, Steyn JL, Turner K, Carretero JA, Yaglioglu O, Su YH, Mlcak R, Spearing SM, Breuer KS, Schmidt MA (2000). Design, fabrication, and testing of a piezoelectrically driven high flow rate micro-pump. In: Applications of ferroelectrics, proceedings of 12th IEEE international symposium, vol 1, pp 297–300.

[6] Suzuki H, Yoneyama R (2003). Integrated microfluidic system with electrochemically actuated on-chip pumps and valves. Sens Actuators B6:38–45.

[7] Yang KS, Chen IY, Chien KH, Wang CC (2004). A numerical study of the nozzle/diffuser micro-pump. In: International conference on MEMS, NANO and smart systems, pp 104–109.

[8] Li B, Chen Q, Lee DG, Woolman J, Carman GP (2005). Development of large flow rate, robust, passive micro check valves for compact piezoelectrically actuated pumps. Sens Actuators A117:325–330.

[9] Benard WL, Kahn H, Heuer AH, Huff MA (1998). Thin-film shapememory alloy actuated micropumps. J Microelectromech Syst 7:245–251.

[10] Francais O, Dufour I, Sarraute E (1997). Analytical static modeling and optimization of electrostatic micropumps. J Micromech Microeng 7:183–185.

[11] Teymoori MM, Abbaspour-Sani E (2005). Design and simulation of a novel electrostatic peristaltic micromachined pump for drug delivery applications. Sens Actuators 117:222–229.

[12] Takao H, Miyamura K, Ebi H, Ashiki M, Sawada K, Ishida M (2003). A thermo-pneumatic in-channel microvalve with PDMS diaphragm for integrated blood examination system on silicon. In: The 12th international conference on solid-state sensors, actuators and Microsystems, vol 1, pp 139–142.

[13] Olsson A, Stemme G, Stemme E (2000). Numerical and experimental studies of flat-walled diffuser elements for valve-less micropumps. Sens Actuators A84:165–175.

[14] Ma HK, Hou BR, Wu HY, Lin CY, Gao JJ, Kau M.C. (2008). Development and application of a diaphragm micro-pump with piezoelectric device, Microsyst Technol (2008) 14:1001–1007 Springer-Verlag 2007.

Paper 2

2. **R.Devarajan**, S. Mahendran, Zainal Ambri Abdul Karim, T.Nagarajan, Analysis of a Valveless Micropump Using Preliminary Characteristics from Fluid Flow, 2nd International Conference on Plant Equipment and Reliability (ICPER 2010).

Analysis of a Valveless Micropump Using Preliminary Characteristics from Fluid Flow

R.Devarajan[1], S. Mahendran[1], Zainal Ambri Abdul Karim[2], T.Nagarajan[2]
[1]Faculty of Mechanical Engineering, Universiti Malaysia Pahang, 26300 Kuantan, Pahang, Malaysia.
Phone: +609-5492223, Fax: +609-5492244. Email: deva@ump.edu.my

[2]Department of Mechanical Engineering,Universiti Teknologi PETRONAS, Bandar Seri Iskandar, 31750 Tronoh, Perak Darul Ridzuan, Malaysia. Phone: +605-3687028, Fax:+605-3656461
Email: nagarajan_t@petronas.com.my , ambri@petronas.com.my

Abstract- **The administration of cooling will need miniaturization of the current pumping system for small scale use. A valve less pump is one of the methods to create a small microscale flowrate pump. It has intake and outlet on the same side. Advances in fluid mechanics are able to capture the working principles of such pumps and give a close approximation of the pump characteristics. The fundamental aspect that a micropump will endure is analysed from fluid mechanics analysis. The sizing and criteria of the pump is set based on fluid equations of mass, momentum and energy. A design is laid out by using computer aided design (CAD) based on the voltage frequency that will be applied to the piezomaterial. The movement of the material due to current will cause the fluid to move as the material will act as a diaphragm. The design moves on to small circuit fabrication so that flow testing is possible. The reading of the small flowrate is analysed and a proper method of designing the valve less pump is gathered.**

I. INTRODUCTION

A novel cooling method with improved pumping performance is crucial to in facing the growing need of the electronic markets.

Micropumps have been developed by using several actuation methods, such as electromagnetic [1], piezoelectric [2],[3],[4],[5],[6],[7],[8], shape memory alloy [9], electrostatic[10],[11], and thermo-pneumatic [12] devices. Most of these micropumps have complex structures and high power consumption. On the contrary, piezoelectric actuation has advantages due to its relatively simple structure and lower power consumption.

In this study, a new type of thin, compact, and light weighed diaphragm micropump will be developed to actuate liquid by the vibration of a diaphragm. The amplitude of vibration by a piezoelectric device produces an oscillating flow and alters the chamber volume by the curvature change of a diaphragm. This enables the pump to function to transfer fluids such as water or air.

A valve less pump consists of two fluid flow rectifying diffuser/nozzle elements which are connected to the inlet and outlet of a pump chamber with a flexible diaphragm. Stemme, [2] proposed the first prototype of valve less pump consisting of a circular cylindrical volume where the top side had a thin brass diaphragm to which a piezoelectric disc was fixed. Its flow rate was 15.6 ml/min. Olssen et al, [3,13] investigated the flow-directing properties of several diffuser elements with different lengths and opening angles for valve less micropumps. Numerical simulations were done by using the Computational Fluid Dynamics program

ANSYS/Flotran. They found that a commercial micropump with a valve can be developed with central actuating as in Figure 1. The drawback is the manufacture and installation of the valve.

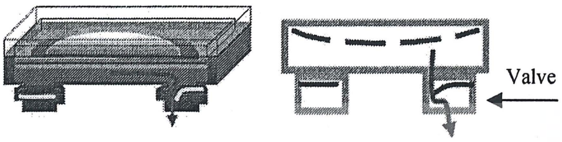

Figure 1 View of SDMP305D Micro-Diaphragm Pump

The vibration amplitude of the piezoelectric device produces an oscillating flow and alters the chamber volume by the curvature change of a diaphragm. When the actuator moves downwards to decrease chamber volume, the outflow will be in one direction by moving from a inlet diffuser to an outlet diffuser. When the actuator moves upwards to increase chamber volume, the fluid flowing into the pump will be in the chamber through the diverged cone, while the fluid outlet will be from the converged cone of the pump as in Figure 2.

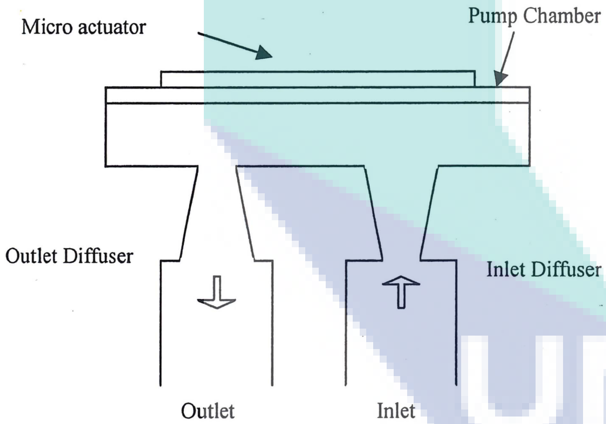

Figure 2 Working Principle of Valveless Micropump

In addition, the actuating force can be enforced by its harmonic resonance of the working fluid with the vibration of a rectangular piezoelectric device, diaphragm, and two cones in the pump chamber. The design of the cones is important in terms of fluid moving into the inlet and going out.

II. MODELING

Based on the boundary equation above and previous research of Ma et al, [14] the opening of the converged cone is set at $d = 0.6$ mm, and flowrate targeted to 0.6 *ml/s*. With the two boundaries predetermined a simulation was targeted by using a CFD tool. This is because the boundary condition is important to represent the flow in the mixer for CFD analysis to begin. The CFD software utilizes the Navier Stokes equations to solve the flow behavior.

$$\frac{\partial \rho}{\partial t} + \frac{\partial}{\partial x_k}(\rho u_k) = 0$$

(1)

$$\frac{\partial \rho u_i}{\partial y} + \frac{\partial}{\partial x_k}(\rho u_i u_k - \tau_{ik}) + \frac{\partial P}{\partial x_i} = S_i$$

(2)

$$\frac{\partial (\rho E)}{\partial y} + \frac{\partial}{\partial x_k}((\rho E + P)u_k + q_k - \tau_{ik} u_i) = S_k u_k + Q_H$$

(3)

Where u is the fluid velocity, ρ is the fluid density, S_i is a mass-distributed external force per unit mass, E is the total energy per unit mass, Q_H is a heat source per unit volume, τ_{ik} is the viscous shear stress tensor and q_i is the diffusive heat flux.

The preliminary model is done as shown in Figure 3 with both cones attached to form the micropump. A moving wall was targeted to oscillate as per the piezomaterial frequency and two outlets, one being an input and the other being an output is modeled in CFD.

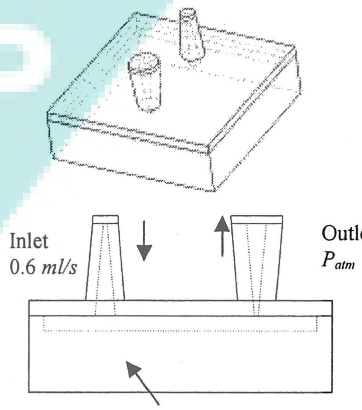

Figure 3 Preliminary Design

III. RESULTS

The results obtained for pressure and velocity show that the pump cavity can deliver the flow as per calculations. Figure 4 and 5 shows the respective simulation. There seem to be a small pressure buildup as the flow is moving from the inlet and exiting the outlet. The amount is small about 18 Pa. This creates very little pressure drop to the system and is seen as an advantage to the design.

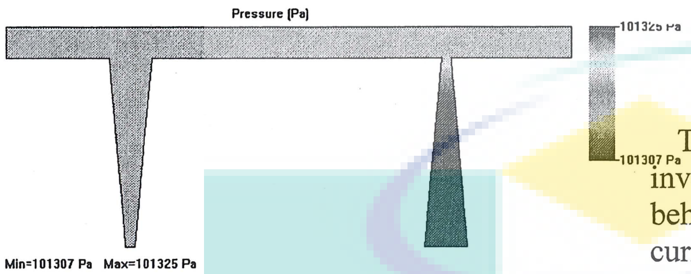

Figure 4 Pressure Readings

In the velocity plot the converged section shows an increase in velocity. This relates to Bernoulli equation where the higher pressure region (inlet) creates a lower velocity and the lower pressure region (converged cone) create higher velocity.

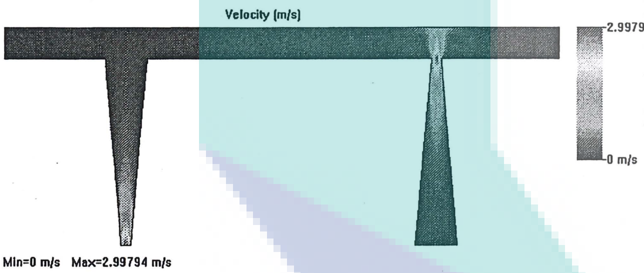

Figure 5 Velocity Readings

Due to the velocity movement, the flow seems to accumulate more in the inlet cone, in the converging section. As seen in Figure 6, the region may cause some fluids with particles to clog the inlet. Small foreign objects will also cause this inlet to be clogged if the flow is too fast. A fillet may help in the future design.

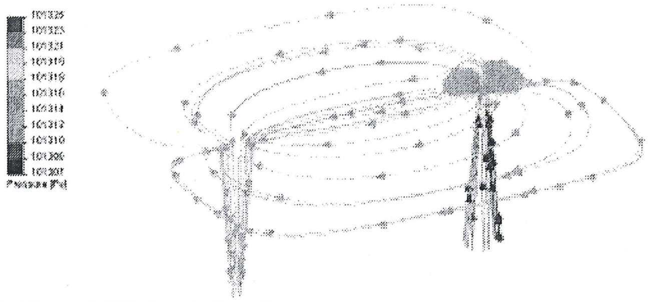

Figure 6 Trajectories of the Flow Moving in the Pump

The other parameters that requires further investigation is on the wall, to ascertain the behavior when piezomaterial is used. The current CFD software used can only enable pressure plots and fluid flow. Hence, more elaborate models will be required to represent the wall as moving per frequency of the model.

As the initial CFD was able to produce flow moving in the micropump body a working circuit is proposed to cater the moving wall of the piezo. The circuit is designed for an initial frequency of 21 kHz. Figure 7 show the final circuit and Figure 8 shows the schematics of the circuits. It consists of integrated circuits, resistors, capacitors and a potentiometer.

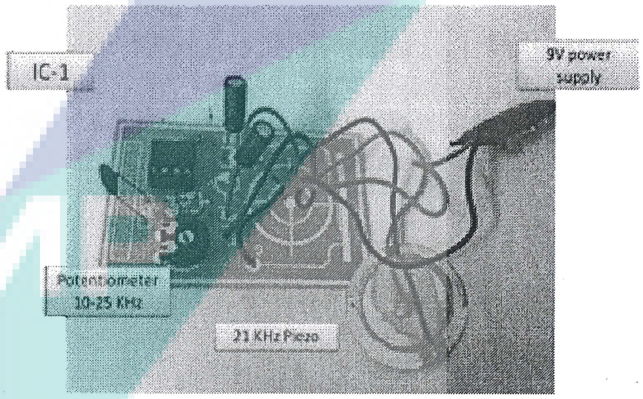

Figure 7 Initial Circuit Designed For the Micropump

The '555 timers' or (IC-1) puts out a continuous stream of rectangular pulses having a specified frequency. Resistor R1 is connected between V_{CC} and the discharge pin (pin 7) and another (R2) is connected between the discharge pin (pin 7), and the trigger (pin 2) and threshold (pin 6) pins that share a common node. Hence, the capacitor is charged through R1 and R2, and discharged only through R2, since pin 7 has low impedance to ground during output low intervals of the cycle, therefore discharging the capacitor.

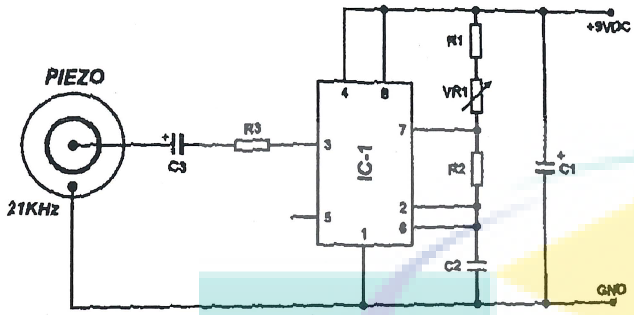

Figure 8 Schematic of the Circuit Used

This piezo, with frequency of 21kHz is used for the micropump initial design as shown in Figure 9 in place of the microactuator as in schematic of Figure 1. A circular shape is used for further analysis as it can be easily fabricated due to the circular piezo shape.

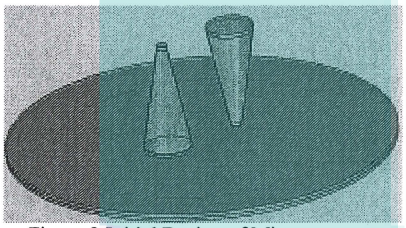

Figure 9 Initial Design of Micropump

IV. Conclusions

As the design has evolved to the electronic circuit development further CFD analysis is targeted so that proper frequency can be controlled for small flow rate of the pump. The final CFD simulation will be used to fabricate a prototype model for initial testing.

Acknowledgment

R.Devarajan would like to thank University Malaysia Pahang for sponsor and financial support for the paper

References

[15] Bo¨hm S, Olthuis W, Bergveld P (1999). A plastic micropump constructed with conventional techniques and materials. Sens Actuators A77:223–228.

[16] Stemme E, Stemme G (1993). A valveless diffuser/nozzle-based fluid pump. Sens Actuators A39:159–167.

[17] Olsson A, Enoksson P, Stemme G, Stemme E (1995). A valve-less planar pump in silicon. In: The 8th international conference on solid-state sensors and actuators, vol 2, pp 291–294.

[18] Koch M, Harris N, Evans AGR, White NM, Brunnschweiler A (1998). A novel micromachined pump based on thick-film piezoelectric actuation. Sens Actuators A70:98–103.

[19] Saggere L, Hagood NW, Roberts DC, Li HQ, Steyn JL, Turner K, Carretero JA, Yaglioglu O, Su YH, Mlcak R, Spearing SM, Breuer KS, Schmidt MA (2000). Design, fabrication, and testing of a piezoelectrically driven high flow rate micro-pump. In: Applications of ferroelectrics, proceedings of 12th IEEE international symposium, vol 1, pp 297–300.

[20] Suzuki H, Yoneyama R (2003). Integrated microfluidic system with electrochemically actuated on-chip pumps and valves. Sens Actuators B6:38–45.

[21] Yang KS, Chen IY, Chien KH, Wang CC (2004). A numerical study of the nozzle/diffuser micro-pump. In: International conference on MEMS, NANO and smart systems, pp 104–109.

[22] Li B, Chen Q, Lee DG, Woolman J, Carman GP (2005). Development of large flow rate, robust, passive micro check valves for compact piezoelectrically actuated pumps. Sens Actuators A117:325–330.

[23] Benard WL, Kahn H, Heuer AH, Huff MA (1998). Thin-film shapememory alloy actuated micropumps. J Microelectromech Syst 7:245–251.

[24] Francais O, Dufour I, Sarraute E (1997). Analytical static modeling and optimization of electrostatic micropumps. J Micromech Microeng 7:183–185.

[25] Teymoori MM, Abbaspour-Sani E (2005). Design and simulation of a novel electrostatic peristaltic micromachined pump for drug delivery applications. Sens Actuators 117:222–229.

[26] Takao H, Miyamura K, Ebi H, Ashiki M, Sawada K, Ishida M (2003). A thermo-pneumatic in-channel microvalve with PDMS diaphragm for integrated blood examination system on silicon. In: The 12th international conference on solid-state sensors, actuators and Microsystems, vol 1, pp 139–142.

[27] Olsson A, Stemme G, Stemme E (2000). Numerical and experimental studies of flat-walled diffuser elements for valve-less micropumps. Sens Actuators A84:165–175.

[28] Ma HK, Hou BR, Wu HY, Lin CY, Gao JJ, Kau M.C. (2008). Development and application of a diaphragm micro-pump with piezoelectric device, Microsyst Technol (2008) 14:1001–1007 Springer-Verlag 2007.

CHAPTER 4

RESULTS AND DISCUSSION

4.0 Modeling

The pumping chamber itself is circular. The model consists of a fluid chamber and a piezoelectric actuator separated by a thin membrane. Common materials were used for the simulations presented here, namely, water, PZT-4, and silicon, respectively. The inlet and outlet ports are located on sides by sides under the chamber and each has a width of 3.5mm and 0.56mm. The pump radius (both the fluid and pump membrane) is 5 mm; the membrane has a thickness of 0.01 mm. The diameter was arbitrarily chosen to approximate existing PZT, the thickness is both a common membrane thickness and a value near the optimal value predicted (Li, S. and Shaochen Chen (2003). "Analytical analysis of a circular PZT actuator for valveless micropumps." Sensors and Actuators A **104**: 151-161). The PZT has a radius of 27 mm and a thickness of 0.48 mm. This size of actuator was chosen to reflect the results of optimization of the piezo/membrane system without fluidic effects. The radius and thickness were optimized simultaneously using both the ANSYS optimization algorithms and manual techniques.

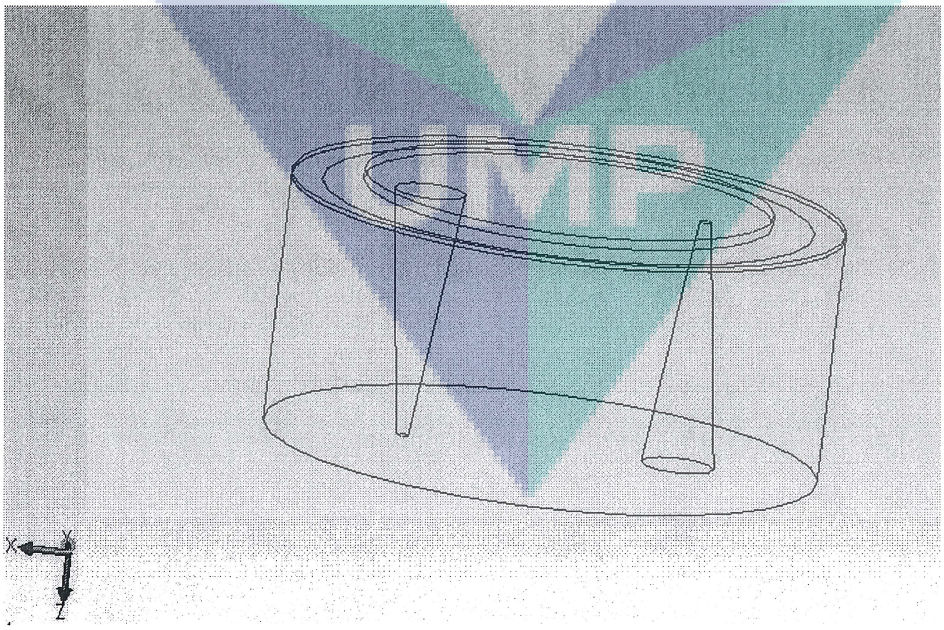

Figure 4.1: Example of modeling of Circular Piezoelectric Micropump

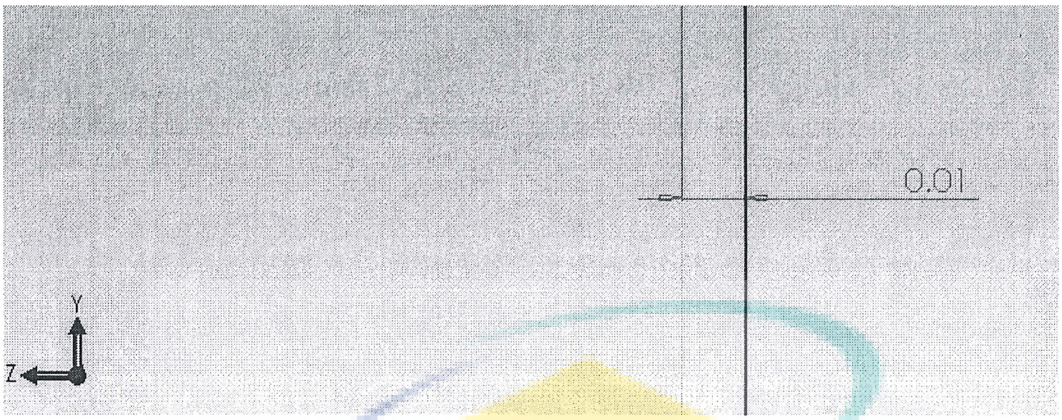

Figure 4.2: Example of modeling of Circular Piezoelectric Micropump Membrane Gap

From the nozzle/ diffuser equation in literature review and fluid mechanics it is known that, the dynamic resistance is minimum at the range of $\theta = 5°$, and the dynamic resistance is maximum when $\theta = 7°$. The flow equation of clearance and pressure distribution of nozzle is given by

$$p = p_1 - \Delta p \frac{\left(\frac{D}{h}\right)^2 - 1}{\left(\frac{D}{d}\right)^2 - 1} \quad (1)$$

And pressure distribution of cone can be expressed as

$$p = p_1 - \Delta p \frac{1 - \left(\frac{d}{h}\right)^2}{1 - \left(\frac{d}{D}\right)^2} \quad (2)$$

Where h, being the cross sectional diameter of the cone. The flow equation of the cone is given by the Bernoulli equation as,

$$\frac{p_1}{\rho g} + \frac{v_1^2}{2g} = \frac{v_2^2}{2g} + \sum \zeta \frac{v_2^2}{2g} \quad (3)$$

Where,

$$v_1 = v_2 \left(\frac{d}{D}\right)^2$$

$\Delta p = p_1 - p_2$
$p_2 = 0$

and,

$$v_2 = \frac{1}{\sqrt{1+\sum\zeta - \left(\frac{d}{D}\right)^4}}\sqrt{\frac{2p_1}{\rho}} \quad (4)$$

4.1 Circuit Design and Calculation

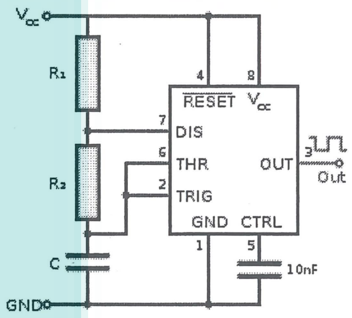

Figure 4.3 : Standard astable circuit NE555 IC timer

Source : http://en.wikipedia.org/wiki/555_timer_IC

To find frequency that being create from this circuit, equation from literature review

$$f = \frac{1}{\ln(2).C.(R_1+2R_2)}$$

and for the high time from each pulse or maximum time for each pulse is using the equation

$$high = \ln(2).(R_1 + R_2).C$$

for the low time or the minimum time from each pulse are using the equation

$$low = \ln(2) . R_2 . C$$

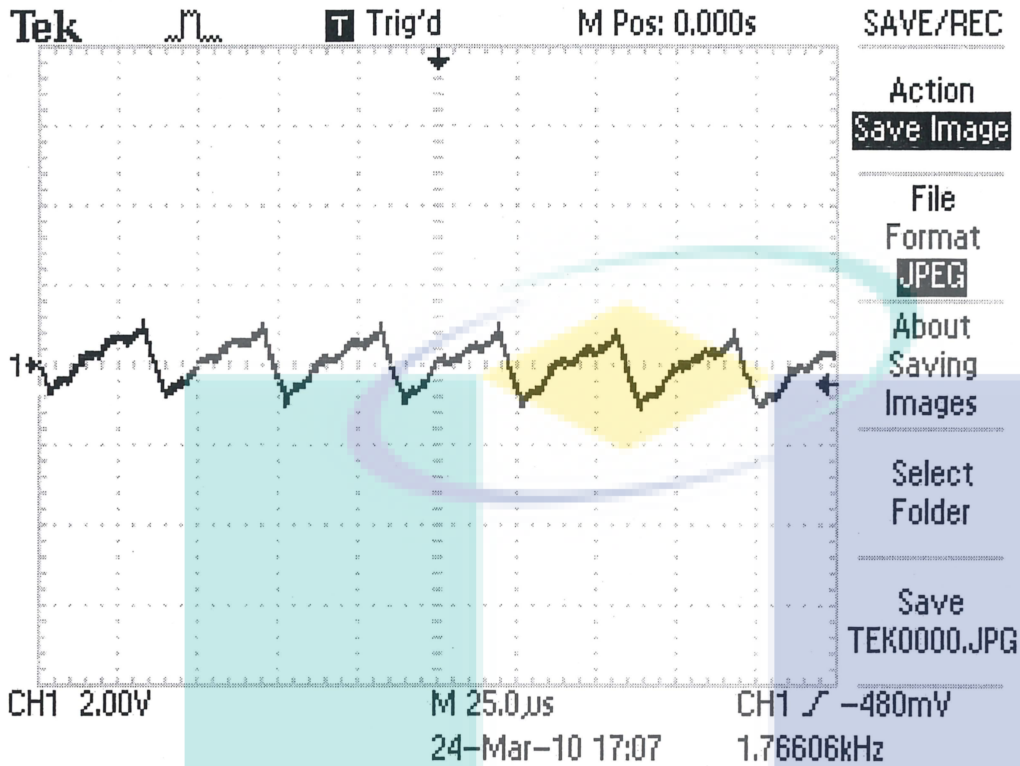
Tek
Trig'd
M Pos: 0.000s
SAVE/REC
Action
Save Image
File
Format
JPEG
About
Saving
Images
Select
Folder
Save
TEK0000.JPG
CH1 2.00V
M 25.0μs
CH1 ∕ −480mV
24−Mar−10 17:07
1.76606kHz

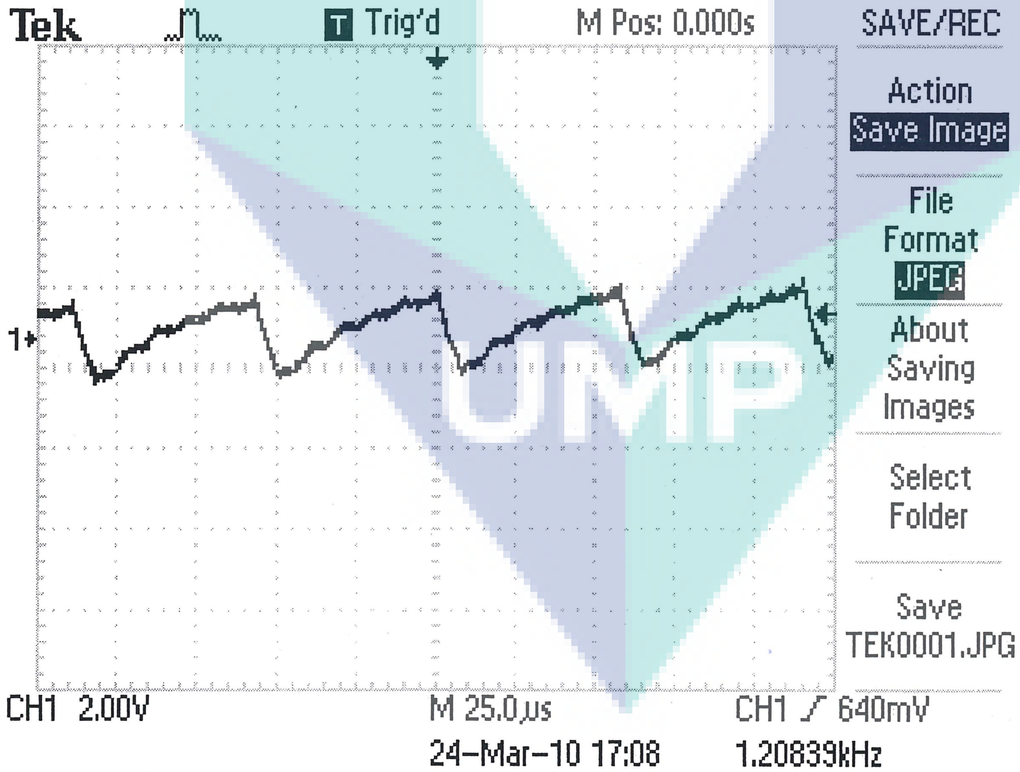
Tek
Trig'd
M Pos: 0.000s
SAVE/REC
Action
Save Image
File
Format
JPEG
About
Saving
Images
Select
Folder
Save
TEK0001.JPG
CH1 2.00V
M 25.0μs
CH1 ∕ 640mV
24−Mar−10 17:08
1.20839kHz

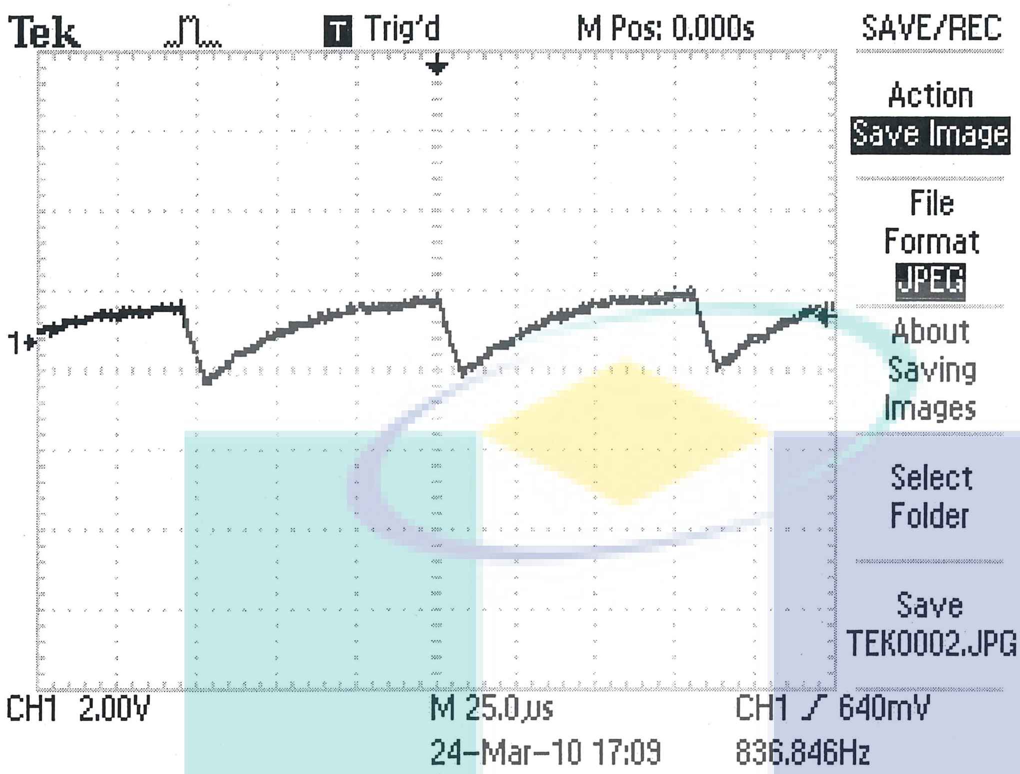

Figure 4.4: Results of Ossciloscope of Piezo Input

1. From the result shown from oscilloscope , when the potential meter at the circuit turn to minimum resistance, the frequency are more higher when the action is opposite the frequency are lower.
2. The results show that when the resistance are change, only the frequency are change but not the amplitude and the means the high of the piezo pulse are stable.

CHAPTER 5

CONCLUSIONS AND RECOMMENDATIONS

5.1 Conclusion

- The dimensions and properties of the PZT disk play a significant role in the actuator performance.
- The micropump was successfully analysed in terms of fluid flow and further research is required to create the working prototype.

5.2 Recommendation

- Find the actual pulse the create from this circuit.
- Find another option or types of circuit design that can used to get the piezo pulse.
- Get the flowrate create from the micropump.
- CFD simulation of the micropump has to done with moving diaphragm as such FLUENT program is targeted.

REFERENCES

- Gravesen, P., Jens Branebjerg, Ole Sondergard Jensen (1993). "Microfluidics - a review." Journal of Micromechanics and Microengineering 3(1993).
- Li, S., and Shaochen Chen (2003). "Analytical analysis of a circular PZT actuator for valveless micropumps."
- Morris, C. J., Fred K Forster (2000). "Optimization of a circular piezoelectric bimorph for a micropump driver."
- H.T.G. van Lintel,F.C.M.van de Pol and S.Bouwstra, A piezoelectric micropump based on micromachining of silicon, *Sensors and actuators,15* (1988).
- E. Stemme and G. Stemme, A valveless diffuser/nozzle-based fluid pump, Sensors and Actuators A,39 (1993).
- A. Olsson, G. Stemme, E. Stemme, A valve-less planar fluid with two pump chambers, Sens. Actuators A 46/47 (1995).
- E.K. Forster, R.L Bardell, M.A. Abramowitz, N.R. Sharma, A. Blanchard, in: Proceedings of IMECE, ASME on Design, Fabrication and Testing of Fixed Valve Micropumps, 1995.
- E.F. Crawley, E.H. Anderson, Detailed models of piezoceramic actuation of beam, J. Intell. Mater. Syst. Struct. 1 (1990).
- A.B. Dobrucki, P. Pruchnicki, Theory of piezoelectric axisymmetric bimorph, Sens. Actuators A 58 (1997).
- D.L. DeVoe, A.P. Pisano, Surface micromachined piezoelectric accelerometers, J. Microelectromech. Syst. 10 (2001).
- Y.L.Cheng and J.H.Lin. 2007. Manufacture of Three-Dimensional Valveless Micropump. *Journal of Material Processing Technology 192-193.*
- L.S. Pan, T.Y. Ng, G.R. Liu, K.Y. Lam and T.Y. Jiang 2001. Analytical solution for the dynamic analysis of a valveless micropump-a fluid membrane coupling. *Sensor and Actuator A93.*
- Y.C.Wang, J.C. Hsu, P.C. Kuo and Y.C. Lee 2008.Loss Characteristic and Flow Rectification Property of Diffuser Valves for Micropump Application. National Cheng. *International Journal of Heat and Mass Transfer.*
- A. Olsson, G. Stemme and E. Stemme. 1996. Diffuser-element design investigation for valve-less pumps. *Sens.Actuator A 57.*
- V.Singhal, S.V. Garimella and J.Y. Murthy. 2004. Low Reynold Number Flow Through Nozzle-Diffuser Elements in Valveless Micropumps. *Sens.Actuator A 113.*
- P. Woias. 2005 Micropumps-past, progress and future. *Sens.Actuator B 105.*
- T.Gerlach. 1998.Microdiffuser as dynamic passive valves for micropump application. *Sens.Actuator A 69.*
- X.N.Jiang, Z.Y. Zhou, X.Y. Huang, Y. Li, Y.Yang and C.Y. Liu. 1998. Micronozzle/ Diffuser Flow and Its Application in Micro Valveless Micropmp. Sens.Actuator A 70.
- S.Li and S.Chen. 2003. Analytical Analysis of a Circular PZT Actuator for Valveless Micropump Sens.Actuator A 104.
- G.K. Arthyuskina. 1973. On the Hydraulic Resistance During Laminar Fluid Flow in Conical Diffuser. Tr. LPI 333.
- B. Wang, X. Chu, E. Li and L. Li. 2006. Simulation and Analysis of a Piezoelectric micropump. Ultrasonic 44.

- A. Olsson, G. Stemme and E. Stemme. 1997. Simulation studies of diffuser and nozzle elements for Valveless Micropump. Int. Conf. Solid-State Sens. Actuator. C.Yamahata, F.Lacharme, and M.A.M. Gijs. 2005. Glass valveles micropump using electromagnetic actuation. Microelectronic Engineering 78-79.

ATTACHMENTS

A. FEM Finite Element Modeling

Test 1

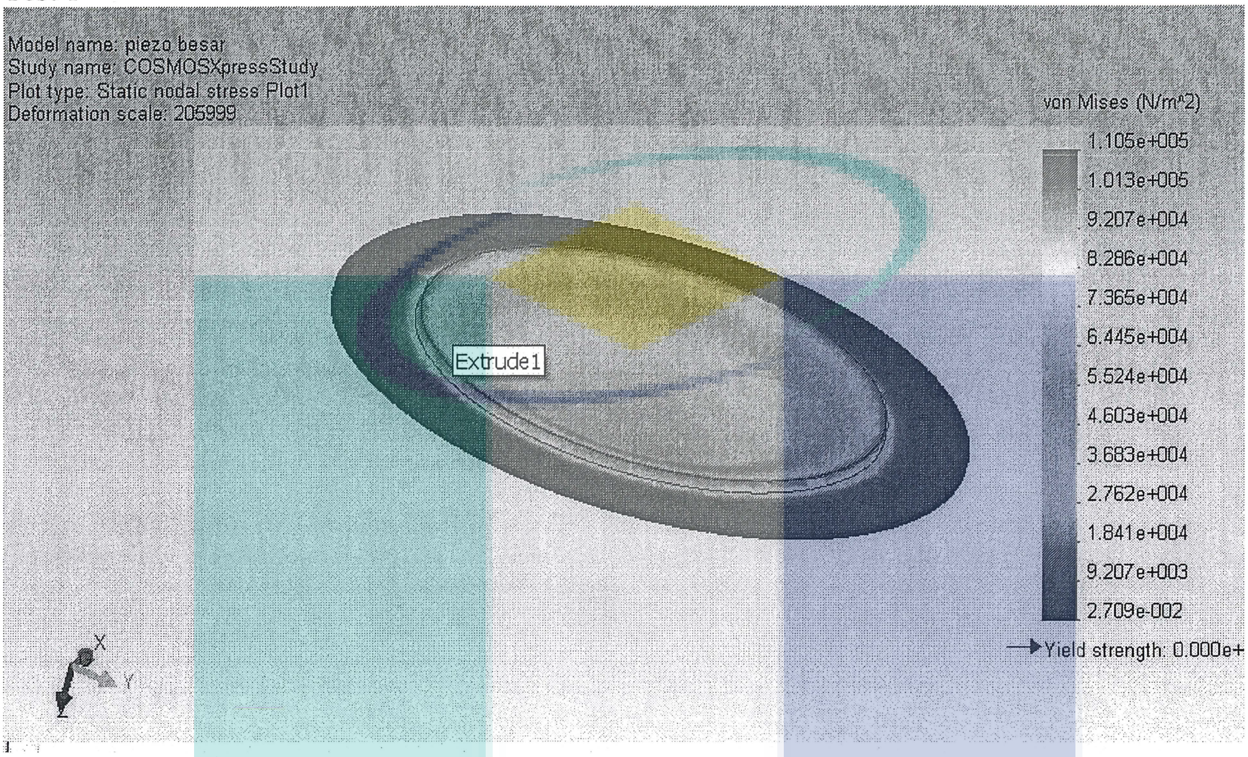

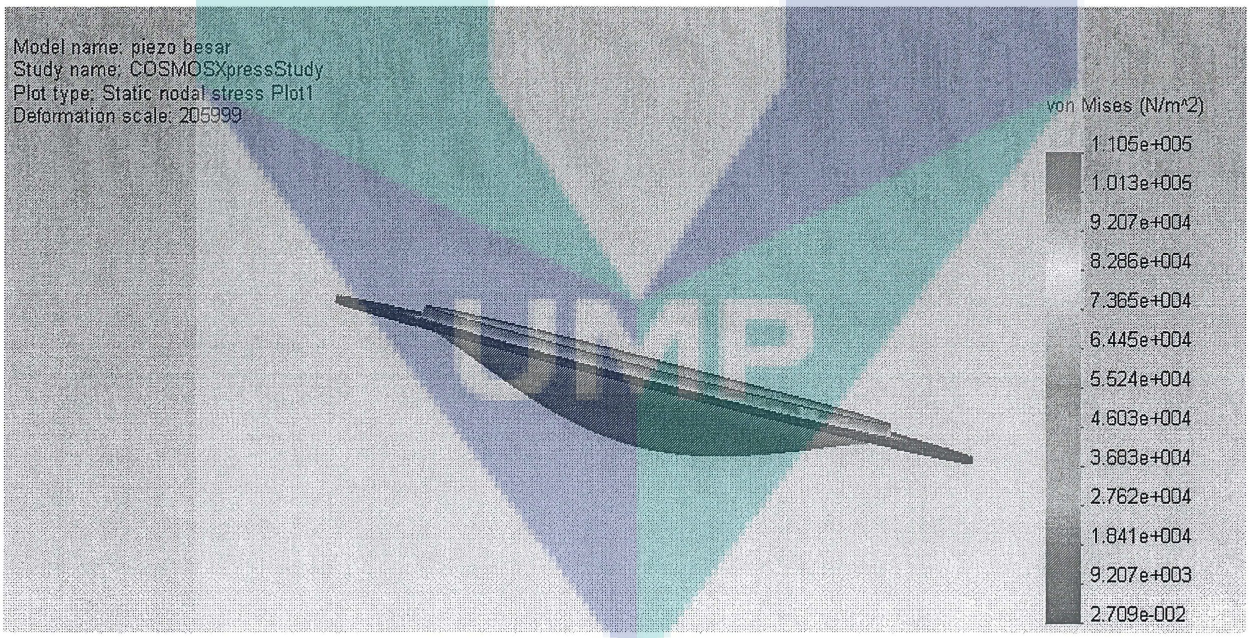

Test 2

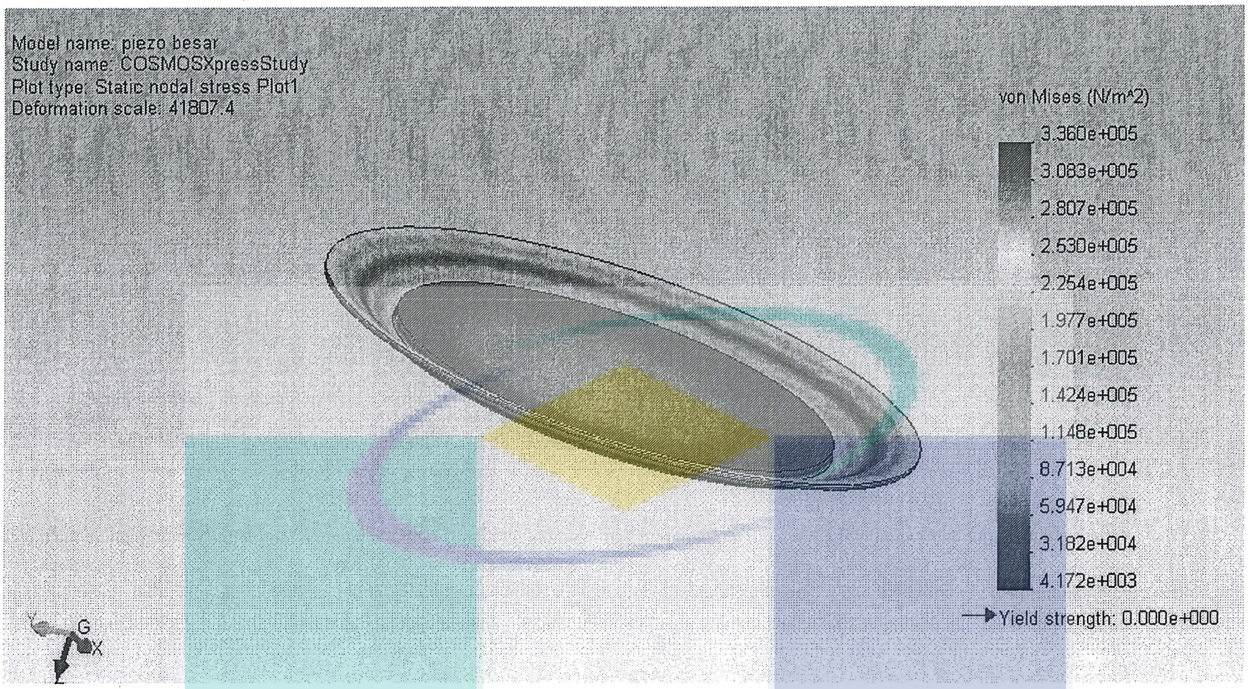
Model name: piezo besar
Study name: COSMOSXpressStudy
Plot type: Static nodal stress Plot1
Deformation scale: 41807.4
von Mises (N/m^2)
3.360e+005
3.083e+005
2.807e+005
2.530e+005
2.254e+005
1.977e+005
1.701e+005
1.424e+005
1.148e+005
8.713e+004
5.947e+004
3.182e+004
4.172e+003
Yield strength: 0.000e+000

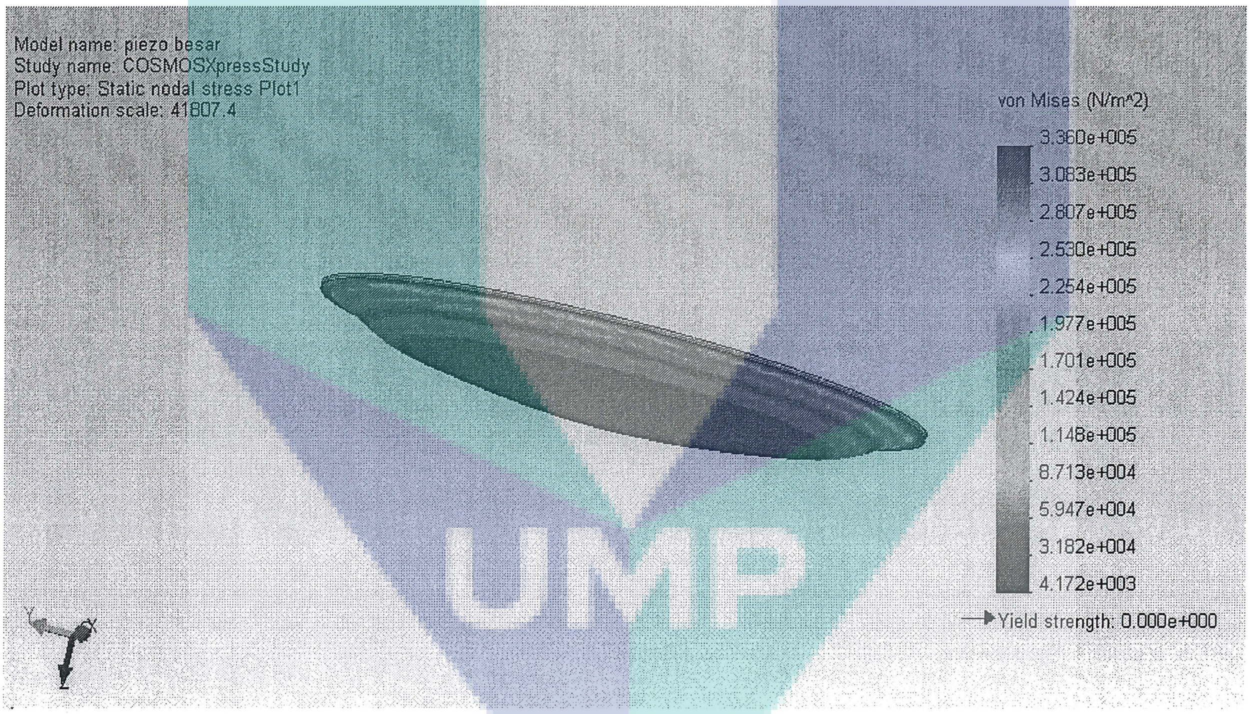
Model name: piezo besar
Study name: COSMOSXpressStudy
Plot type: Static nodal stress Plot1
Deformation scale: 41807.4
von Mises (N/m^2)
3.360e+005
3.083e+005
2.807e+005
2.530e+005
2.254e+005
1.977e+005
1.701e+005
1.424e+005
1.148e+005
8.713e+004
5.947e+004
3.182e+004
4.172e+003
Yield strength: 0.000e+000

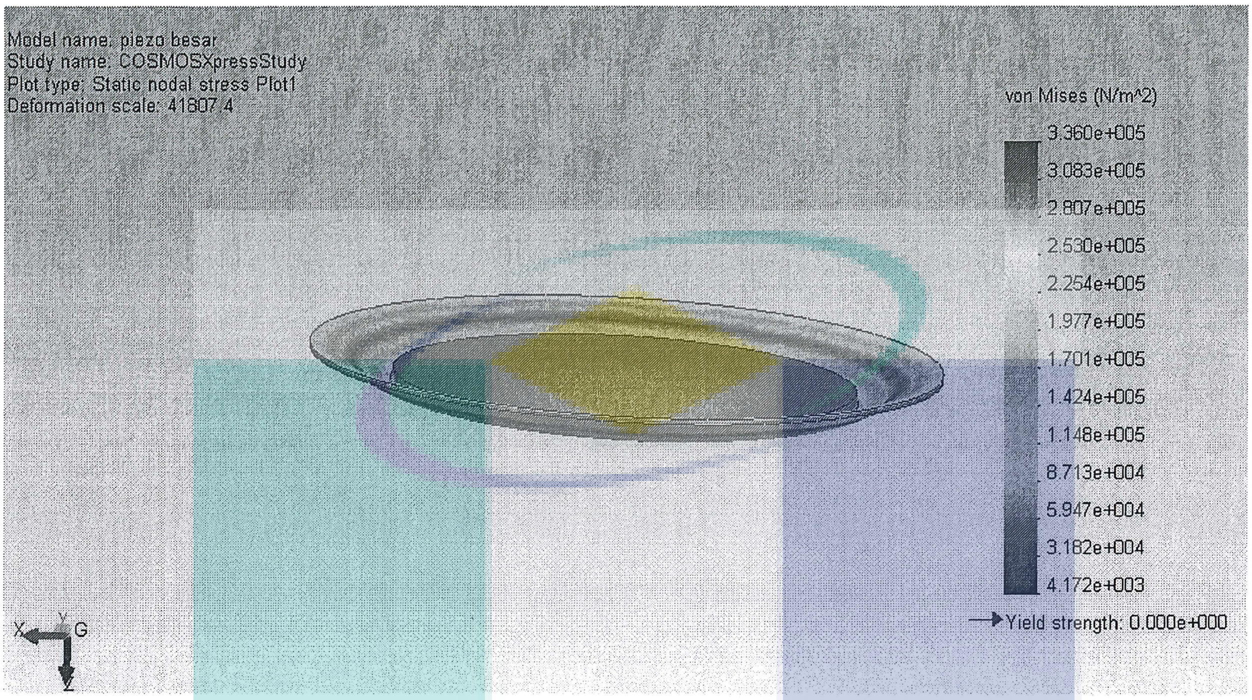
Model name: piezo besar
Study name: COSMOSXpressStudy
Plot type: Static nodal stress Plot1
Deformation scale: 41807.4
von Mises (N/m^2)
3.360e+005
3.083e+005
2.807e+005
2.530e+005
2.254e+005
1.977e+005
1.701e+005
1.424e+005
1.148e+005
8.713e+004
5.947e+004
3.182e+004
4.172e+003
Yield strength: 0.000e+000

D. Equipments

Developed Piezoelectric Circuit

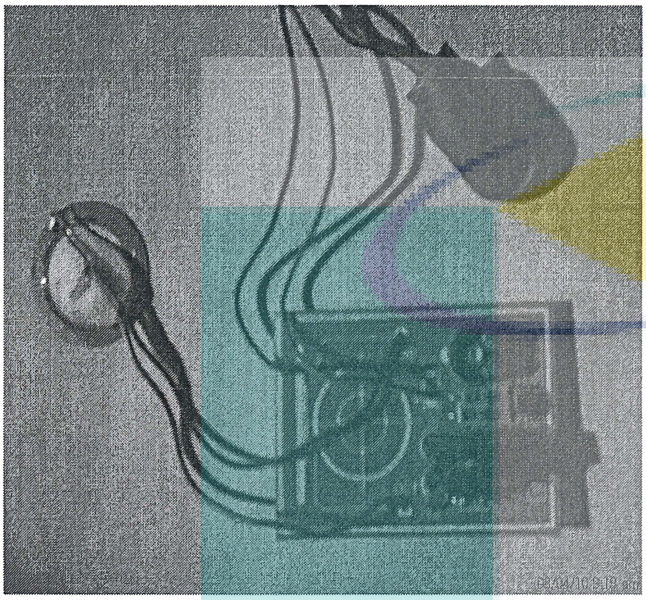

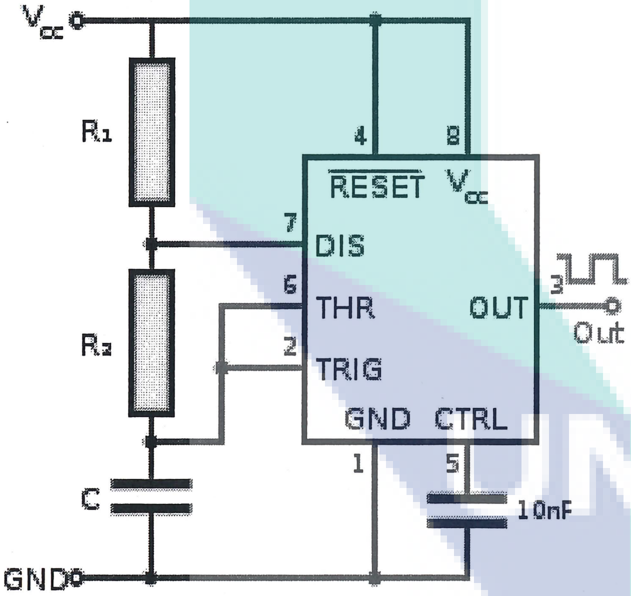

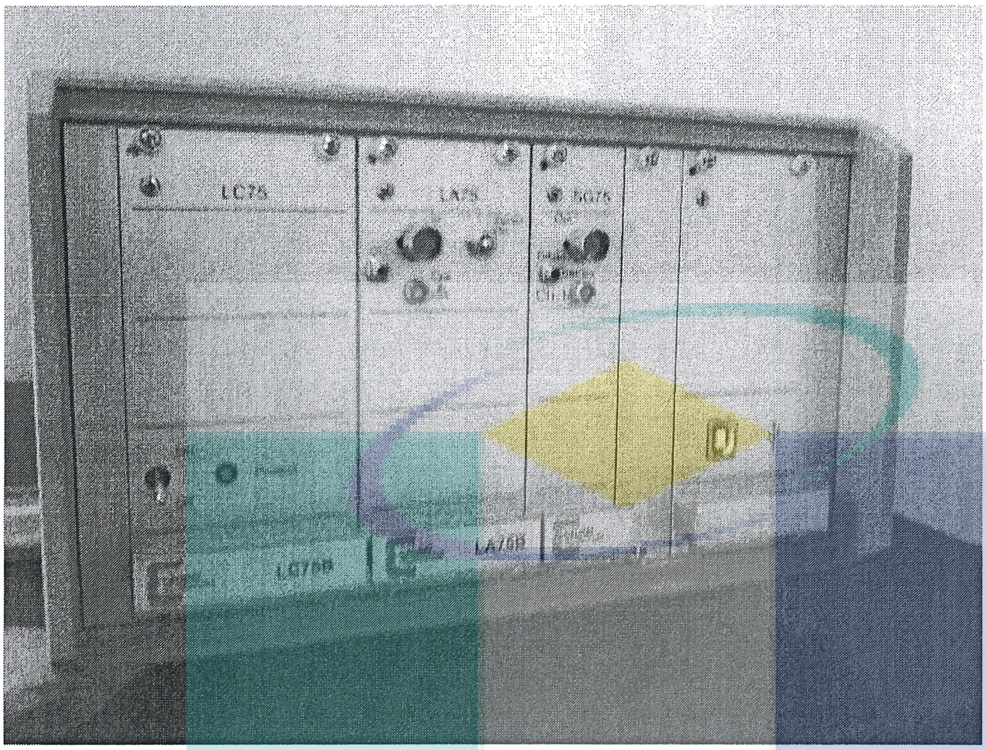

Linear Amplifier LA 75B-1

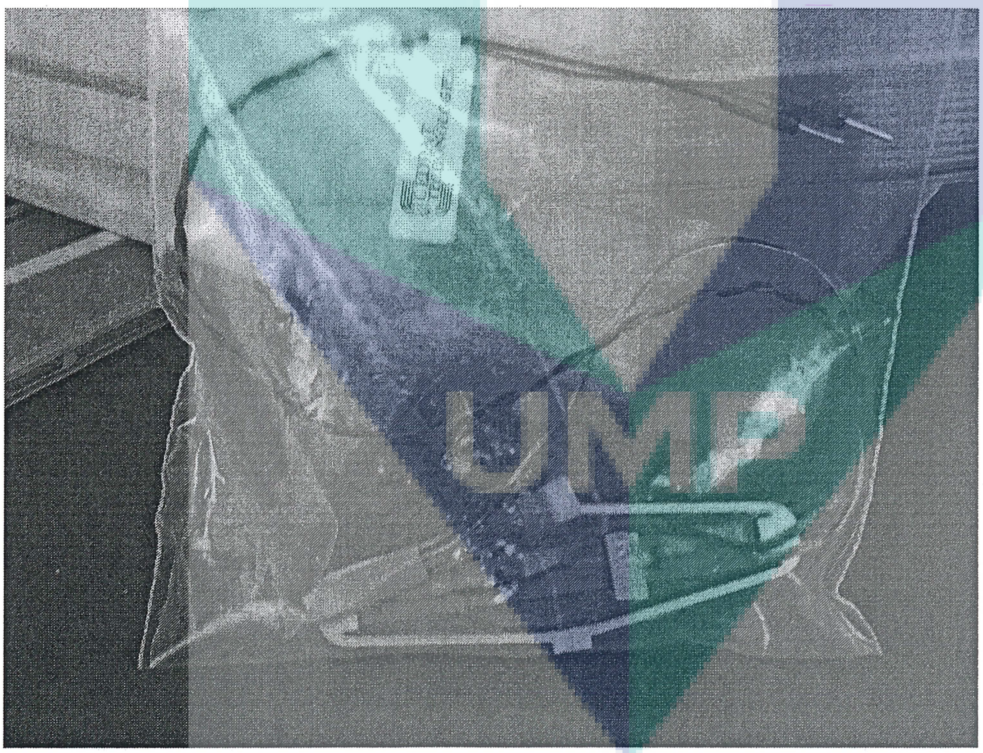

Amplified Piezo Actuator APAm-SG and Displacement 400 micron Strain Gauge

E. GANTT CHART

Activities / Quarter (Yrs)	2009				2010				2011			
	1st	2nd	3rd	4th	1st	2nd	3rd	4th	1st	2nd	3rd	4th
Literature Review	■	■										
Micropump Selection		■	■	■								
Designing and fabrication of the Prototype					■	■	■					
Modeling							■	■				
Experiments Works								■	■			
Results and Verification									■	■		
Report writing			■	■	■	■	■	■	■	■	■	■